In vitro regeneration of primary cell cultures of cortex from postnatal grey short-tailed opossum Monodelphis domestica

Pongrac, Marta

Master's thesis / Diplomski rad

2021

Degree Grantor / Ustanova koja je dodijelila akademski / stručni stupanj: **University of Rijeka / Sveučilište u Rijeci**

Permanent link / Trajna poveznica: https://urn.nsk.hr/urn:nbn:hr:193:913775

UNIVERSITY OF RIJEKA

DEPARTMENT OF BIOTECHNOLOGY

Master's program

Biotechnology in medicine

Marta Pongrac

In vitro **regeneration of primary cell cultures of cortex from postnatal grey short-tailed opossum** ***Monodelphis domestica***

Master's thesis

Rijeka, 2021

UNIVERSITY OF RIJEKA

DEPARTMENT OF BIOTECHNOLOGY

Master's program

Biotechnology in medicine

Marta Pongrac

In vitro **regeneration of primary cell cultures of cortex from postnatal grey short-tailed opossum** ***Monodelphis domestica***

Master's thesis

Rijeka, 2021

Mentor: Jelena Ban, PhD, Assist. Prof.

Co-mentor: Miranda Mladinić Pejatović, PhD, Full Prof.

SVEUČILIŠTE U RIJECI

ODJEL ZA BIOTEHNOLOGIJU

Diplomski sveučilišni studij

Biotehnologija u medicini

Marta Pongrac

In vitro* regeneracija primarnih staničnih kultura korteksa postnatalnih oposuma *Monodelphis domestica

Diplomski rad

Rijeka, 2021.

Mentor rada: doc. dr. sc. Jelena Ban

Komentor rada: izv. prof. dr. sc. Miranda Mladinić Pejatović

Acknowledgments

I wish to thank my dear mentor Assist. Prof. Jelena Ban for her guidance and her generous sharing of knowledge and endless support during my master thesis and work in the laboratory. Also, I would like to thank my co-mentor Full Prof. Miranda Mladinić Pejatović for the opportunity to join the laboratory and for professional advice and leadership. I wish to thank Dr. Dan Cojoc for his guidance during the calcium imaging method setup, obtaining and analyzing the results.

I am extremely thankful to have had the opportunity of working alongside and under careful guidance of Ph.D. students Antonela Petrović and Ivana Tomljanović. Your advice, help and shared knowledge will always be in my mind and I will always look up to you. The biggest thank you to Matea Ivaničić for being by my side since the beginning of my university education and for being my laboratory partner and support system. You all have made my laboratory experience and learning a really special, positive and loving environment!

I wish to thank my family and friends for their support, patience and motivation.

Master's thesis was defended on 23rd July, 2021

in front of the committee:

1. Assoc. Prof. Ivana Munitić

2. Assoc. Prof. Dinko Mitrečić

3. Full Prof. Miranda Mladinić Pejatović

4. Assist. Prof. Jelena Ban

This thesis has 67 pages, 23 figures, 6 tables and 51 references.

Abstract

Mammalian central nervous system (CNS) begins to develop in early embryonal period. CNS has then the ability to regenerate itself, while soon after birth, regeneration stops. Opossum *Monodelphis domestica* is a unique model for investigating CNS regeneration because it is born at a very immature stage of CNS development. Opossum has a unique possibility to successfully regenerate spinal cord after injury in the first two weeks of their postnatal development. Regenerative capacity abruptly declines after that period and is completely lost in mature organism. Two significantly different ages of opossum at postnatal days (P)3-5 and P16-18 have different cell environment and gene profile which determine the capability of spinal cord regeneration after injury. Apart from spinal cord, opossum cortex and capability of its regeneration remain unexplored. Aim of this thesis is to establish and characterize primary cell cultures of opossum cortex, in order to explore the CNS cell composition, maturation and regeneration at a molecular basis *in vitro.* Immunofluorescence was used to characterize the cell composition and expression of markers linked to CNS maturation and regeneration. Scratch assay was used to study the response of cells and of their environment to injury. Calcium imaging method was used to study the maturation of cells and cell networks formed in cultures, as well as activity recovery after injury. Primary cortical cell cultures of neonatal opossum can be maintained up to a month *in vitro*. P3-5 cultures consist of 93% of neurons and almost 50% of cells positive for progenitor marker SOX2, while P16-18 cultures consist of 80% of neurons and 30% of $SOX2^{+}$ cells. An interesting discovery is the co-expression of neuronal marker with SOX2, which was not investigated in opossum before. *In vitro* cortical cell culture temporal maturation correlates with the maturation of opossum cortex *in vivo.* Spontaneous activity of neurons and neuronal networks is observed in 7th day *in vitro* (DIV7) of both age groups (P3-5 and P16-18). After the injury, neurons regenerate axons which after 48 hours connect the opposite sides of the injury. A reduction in injury width, as well as glial-scar-like formation is visible in DIV10 cultures of both ages. By calcium activity, it has been shown that 48 hours after the injury, neuronal networks of the opposite sides of the injury are reconstituted and synchronized. These results contribute to understanding of opossum cortex maturation, as well as cell microenvironment on the cortex regeneration upon injury. Integration of results may contribute to better understanding of cell adaptation on pathophysiological conditions of mammalian cortex.

Key words *primary cell cultures, opossum, injury, CNS regeneration, calcium imaging*

Sažetak

Središnji živčani sustav (SŽS) sisavaca počinje s razvojem u ranom embrionalnom periodu. Tada SŽS posjeduje sposobnost regeneracije, dok se ubrzo nakon rođenja sposobnost regeneracije gubi. Oposum *Monodelphis domestica* jedinstven je model za istraživanje regeneracije SŽS-a jer se rađa u vrlo nezrelom stadiju razvoja SŽS-a. Oposum posjeduje sposobnost regeneracije leđne moždine nakon ozljede tijekom prva dva tjedna postnatalnog razvoja. Sposobnost regeneracije naglo pada nakon tog perioda te se u potpunosti gubi u zrelom organizmu. Dvije značajno različite dobi oposuma, postnatalni dan (P)3-5 i P16-18 sadrže različiti stanični okoliš i genski profil koji uvjetuju sposobnost regeneracije leđne moždine nakon ozljede. Za razliku od leđne moždine, korteks mozga i sposobnost njegove regeneracije u oposumu ostaju neistraženi. Cilj ovog rada je uspostava i karakterizacija primarnih staničnih kultura korteksa oposuma, kako bi se omogućilo istraživanje staničnog sastava, maturacije i regeneracije SŽS-a na molekularnoj bazi *in vitro*. Metodom imunofluorescencije, karakterizirao se stanični sastav i ekspresija markera povezanih s razvojem SŽS-a i regeneracijom. Izazivanjem ozlijede *in vitro,* istražio se odgovor stanica i staničnog okoliša na ozljedu. Funkcionalnim ispitivanjem oslikavanja kalcija, proučila se zrelost stanica i staničnih mreža formiranih u staničnim kulturama, kao i ponovno uspostavljene aktivnosti nakon ozlijede. Primarne stanične kulture korteksa neonatalnog oposuma mogu se održavati do mjesec dana u *in vitro* uvjetima. Stanične kulture P3-5 oposuma sadrže 93% neurona i gotovo 50% stanica pozitivnih na marker progenitora (SOX2), dok stanične kulture P16-18 oposuma sadrže 80% neurona i 30% $SOX2^+$ stanica. Zanimljivo otkriće predstavlja koekspresija markera neurona i progenitora (SOX2), koja nije do sada istražena u oposumima. *In vitro* maturacija staničnih kultura korteksa vremenski korelira sa maturacijom korteksa oposuma *in vivo.* Spontana aktivnost neurona i mreža neurona uočena je već u 7. danu u kulturi (DIV7) za obje dobi (P3-5 i P16-18). Nakon ozljede, neuroni regeneriraju aksone koji već 48 sati nakon ozljede povezuju suprotne strane ozljede. Smanjenje promjera ozljede, kao i formiranje staničnih struktura sličnim glijalnom ožiljku je uočeno već u DIV10 kulturama obiju dobi. Oslikavanjem aktivnosti kalcija, potvrđeno je da su 48 sati nakon ozljede neuronalne mreže između suprotnih strana ozljede ponovno uspostavljene i sinkronizirane. Ovi rezultati doprinose razumijevanju maturacije korteksa oposuma, kao i utjecaju staničnog mikorookoliša na regeneraciju korteksa nakon ozljede. Integracija dobivenih rezultata mogla bi doprinijeti boljem razumijevanju prilagodbe stanica na patofiziološka stanja u korteksu sisavaca.

Ključne riječi *primarne stanične kulture, oposum, ozljeda, regeneracija SŽS-a, oslikavanje aktivnosti kalcija*

Contents

1. Introduction

1.1. Central nervous system injury

Central nervous system (CNS) injury in mammals leads to severe consequences due to the intrinsic inability of mature CNS to regenerate and reconstruct its functional cell networks. Moreover, disrupted neuronal connectivity and signal transduction in damaged regions progressively leads to cell death and neurodegeneration. Considering the onset time, the CNS injury outcomes can be divided into two stages – the primary insult and the secondary insult. The primary insult, also known as the primary (or mechanical) damage, occurs at the impact time, while the secondary insult occurs with delayed clinical presentation[1].

Immediate effect of the CNS tissue damage is the impaired blood flow, which depletes the oxygen levels in the cells, leading to ischemia-like conditions. This leads to the switch from aerobic to anaerobic metabolism and increased membrane permeability. Insufficient energy level diminishes the energy-based functions in cells, such as energy-dependent membrane ion pumps activity. Cell membranes become depolarized and release a vast amount of excitatory neurotransmitters, activating α-amino-3-hydroxy-5-methyl-4-isoxazolepropionic acid (AMPA) receptors and voltage-dependent calcium and sodium channels. Consequently, calcium (Ca^{2+}) and sodium (Na^{+}) ions influx activate a cascade of intracellular processes. Activated proteases, phospholipases and lipid peroxidases raise free radical and free fatty acid levels. Furthermore, activated caspases and endonucleases induce structural changes of DNA, inhibition of DNA repair, DNA fragmentation and cell death. Cell death can occur mainly in two ways: apoptosis or necrosis. If the energy supply is sufficient, cells undergo apoptosis. In apoptosis, DNA condensates, nuclear membranes disintegrate and undergo lysis. Alternatively, if the damage is too big and there is not enough energy, necrosis occurs. Necrosis is characterized with substantial

release of excitatory neurotransmitters and metabolic collapse followed by an inflammatory response and glial scar formation[1].

Following the mechanical CNS injury, damaged and surrounding cells release pro-inflammatory cytokines and signal molecules which activate the cells and induce local neuroinflammation. Interleukin (IL)-1 upregulates the intermediate filament production in astrocytes, which results in extended astrocytic processes and hypertrophy. Moreover, IL-6 induces neural progenitor cell (NPC) differentiation into astrocytes. Hypertrophic, reactive astrocytes proliferate and migrate to the lesion site, filling the space around dead or dying neurons in a process called reactive astrogliosis[2,3]. Microglia and macrophages proliferate and accumulate at the lesion site, as well. The damage induces changes in extracellular matrix (ECM), which results in secretion of proteoglycans, laminin and fibronectin[3]. This complex process of reactive astrogliosis followed with formation of fibrotic tissue is called a glial scar. Glial scar represents a physical and chemical barrier, which contributes to secondary damage to nearby cells and inhibits the recovery[2]. Still, neuroprotective effect of glial scar has been investigated. The lesion site gets sealed, which prevents further CNS damage. Glial scar also controls blood flow, modulates immune response and stimulates generation of new neurons[4].

1.2. Central nervous system regeneration

Mature mammalian CNS has extremely limited capacity of regeneration after injury. Mature cortical neurons cannot adequately react to the insult due to the extracellular inhibitory signals and reduced intrinsic capacity to grow. Moreover, structural plasticity of the brain declines with the CNS maturation. Yet, recent research has shown that mature CNS in rodents, non-human primates and other mammals retains some capability to regenerate after the injury[5].

1.2.1. Generation of new cells in the adult brain

In the adult mammalian brain, new cells are produced through differentiation of neural progenitor cells, derived from embryonic stem cells (ESC). In the terminology of neural progenitor cells, overlapping terms indicating same cell types are often used. Therefore, in this work, the terminology described in Martínez-Cerdeño and Noctor's[6] article will be used. NPCs can give rise to glial and neuronal cell types in the CNS (Figure 1). They are present in developing, but also in adult CNS. NPCs can be divided by developmental potential, location, gene expression and morphology, and have restricted self-renewal capacity. They give rise to lineage-specific progenitors that can further differentiate into a single cell lineage.

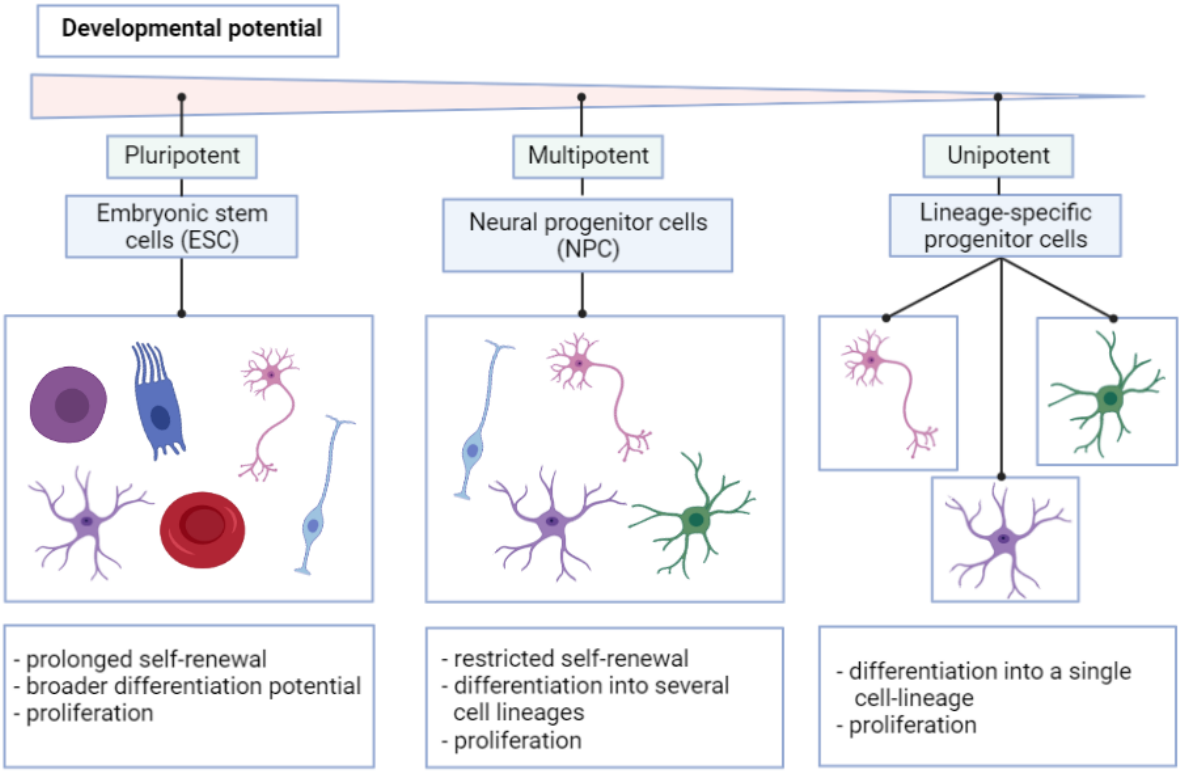

Figure 1 Schematic overview of progenitor cells in the CNS. Progenitors cells are divided by their developmental potential, as well as by cell lineage they can give rise to. Illustration was created with BioRender.com.

Neurogenesis is a process in which neurons are generated through the division of NPCs and their differentiation into neuron-specific progenitors. They give rise to immature neurons. They subsequently develop into fully functional and mature neurons which integrate into and modify existing neuronal networks[7]. In gliogenesis, NPCs differentiate into glial progenitors, which differentiate into astrocytes, oligodendrocytes and ependymal cells[8]. Both neurogenesis and gliogenesis in the adult brain are tightly controlled and correlated processes by which new cells are generated.

Mammalian CNS progenitors are highly heterogeneous cells and depend on site-specific brain regions, as well as conditions and permissiveness of their surrounding microenvironment. The majority of adult brain neurogenesis occurs in the subventricular zone (SVZ) of the lateral ventricles, olfactory bulb and the subgranular zone (SGZ) of dentate gyrus of hippocampus. But recent research has shown progenitors isolated from cortex[9], substantia nigra[10], amygdala[11] and others, suggesting the possibility of NPC distribution throughout the brain. However, permissiveness of the microenvironment differs across different brain regions and affects the progenitor cell ability to produce mature, functional cells. SVZ and hippocampus have been extensively investigated and are described as germinative areas in various mammals that retain the ability to regenerate throughout life[7].

In the adult SVZ and SGZ, cells are derived from radial glia(-like) cells (RGC). Radial glia are derived from neuroepithelial cells (NEC) and populate the brain during embryonic development. They retain the ability to self-replicate and differentiate into several cell lineages – astrocytes, oligodendrocytes and neurons[8]. They are the major population of progenitor cells during neurogenesis, which suggests that they generate new neurons directly. RGCs divide asymmetrically into one RGC and one neuron. Newly formed neurons reduce their radial processes and translocate to their target

position following the RGC-formed scaffold[12]. Neurogenesis precedes gliogenesis, and most neurogenic RGCs disappear when gliogenesis begins. RGC number diminishes in the adult brain, implying the adult neurogenesis may be insufficient, also because of RGC differentiation into astrocytes and oligodendrocytes[13].

Generation of new cells in the adult brain relies on conditions and microenvironment of the specific region, so the capacity of neurogenesis and gliogenesis can be influenced with environmental factors. In rodent hippocampus, neurogenesis can be decreased with drug abuse[14] and stress[15]. In contrast, cell proliferation can be enhanced by physical activity[16] and in the presence of dying hippocampal neurons after the stroke, brain tumor or injury[17,18]. Apart from mechanical lesions, excitotoxicity stimulates the proliferation of progenitor cells into neurons[18].

1.2.2. Generation of new cells in the adult brain after an injury

Adult neurogenesis promotes neural repair of damaged tissue after a traumatic brain injury (TBI). Dying cells and nearby cells release stress-related cytokines and growth factors, inducing enhanced proliferation of progenitor cells[18]. Dash et al.[18] have shown that the rate of cell production in hippocampus increases after TBI. Newly produced cells express markers of differentiated and mature granular neuron markers. Chirumamilla et al.[19] have shown that after an fluid percussion injury, cell proliferation is induced in SVZ and hippocampus and that the majority of newly generated cells express markers of astrocytes and microglia. Furthermore, Ramaswamy et al.[17] have investigated controlled cortical impact and found induced cell proliferation in striatum, dorsal SVZ and subcortical structures connected to the lesion area. Newly formed cells migrated from SVZ to lesion site and expressed markers for neuroblasts, immature neurons and astrocyte-like stem cells.

1.2.3. Limited capacity of neuronal regeneration

Axonal regeneration in CNS is inhibited by intrinsic and extrinsic factors, which disrupt the regeneration capacity after an injury. Aguayo et al.[20] have shown that injured CNS axons can grow into grafted permissive substrates, which opened the study of environmental permissiveness for axonal growth. Numerous inhibitory factors have been revealed since, associated with axonal components, myelin debris and glial scar. Chondroitin sulfate proteoglycans (CSPGs) are one of the main regeneration inhibitors, upregulated during glial scar formation. CSPGs are produced by reactive astrocytes and secreted extracellularly, inhibiting axonal growth and CNS regeneration[21].

Axotomy is a term describing the neuronal axon splitting into two or more parts, in a way that the cell body becomes disconnected from its terminal ends. Injured neurons initiate the growth cone (GC) sprouting and axon elongation to reach their target location and regenerate. Elongation occurs through polymerization of actin filaments[22]. This process requires proteins and lipids, which can be transported from pre-existing sources in cell and also *de novo* synthesized. Axon injuries that occur further from soma require more energy due to the transport of the molecules needed for axonal extension and regeneration. Therefore, to regenerate, neurons have to upregulate their metabolism and protein synthesis. This results in shift from catabolic to anabolic processes, promoting *de novo* synthesis of molecules. In contrast, atrophic neurons have reduced arborization and catabolic processes prevail[23].

Regrowth of axons following the injury involves extension following GC formation, much like at embryonic stages of CNS development. The critical difference between embryonic GCs and GC formation following injury is the sprouting location. In the embryonic development, GCs sprout from neuronal cell bodies or branchpoints, while after an injury they sprout from injured axon ends. Moreover, developing neurons have smaller bodies and

need to grow shorter distances than in the adult CNS. Injured axons in the adult CNS often retract from the lesion site or fragment due to the inability to survive, while some initiate immediate local sprouting, contributing to functional improvements after injury[23].

1.3. Calcium activity in CNS development and regeneration

Calcium activity of neural circuits, in addition to single-cell intracellular calcium oscillations in neurons and glial cells can contribute to deeper understanding of the CNS development, as well as CNS reconstitution upon injury. Spontaneous electrical and chemical activity in CNS happens even before first synapses form and this early activity influences neuronal differentiation and migration. Neuronal progenitors and immature neurons grow, extend their processes and start forming synaptic connections. Spontaneous electrical activity is then modulated and synchronized, and functional local circuits are formed[24].

Intracellular calcium levels regulate the key processes of CNS formation and regulation, such as neuronal development, proliferation, migration, differentiation and cell survival. Calcium transients also contribute to regulation of dendritic growth and arborization, axonal pathfinding, differentiation into neuronal subtypes[25] as well as neuronal plasticity in developing and mature CNS. Neuronal plasticity enables modulation of forming or already existing neuronal connections as a response to environmental signals. After a signal is detected, adequate response of CNS is critical for reconstitution of existing circuits and regeneration processes[26].

Intracellular calcium levels determine the initial stages of CNS regeneration. Regeneration depends on three steps – resealing of the severed membrane, formation of new GCs (pathfinding) and regeneration of new processes. *In vitro* experiments with lowered calcium levels, showed

slower membrane sealing and GC formation in rodents. However, with elevated intracellular calcium levels, neuronal regeneration of GCs is also impaired[27]. Proper calcium homeostasis is therefore one of the key processes involved in CNS regeneration.

1.4. Identification of CNS cells

1.4.1. Developmental markers for CNS cells

CNS originates during embryonic development from NECs. NECs divide symmetrically and form neural tube, after which they generate RGCs. RGC soma remains in the VZ and stretches to the outer surface of neural tube. Afterwards, neurogenesis and gliogenesis occur by which RGCs further differentiate. Microglia also populate the brain during embryonic development, but they originate from primitive yolk-sac progenitors[28]. At every developmental stage, CNS cells express different gene profile. Translation products of these genes at various developmental points have become standard markers for cell identification, visualization and characterization (Figure 2).

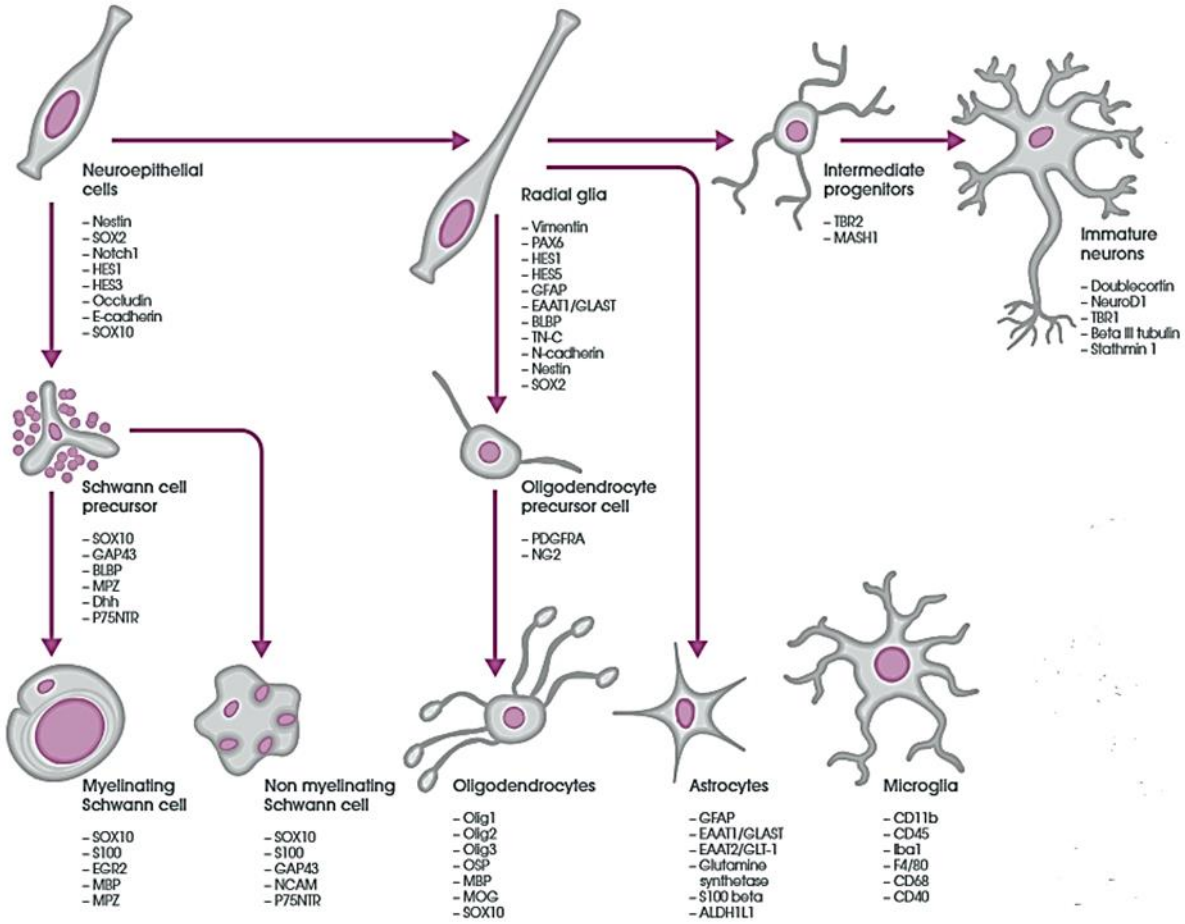

Figure 2 Schematic illustration of CNS cell types and their corresponding molecular markers. Illustration source: abcam.com/neuralmarkers.

NECs and RGCs have characteristic bipolar morphology and express genes necessary for proliferation and differentiation of progenitor cells, such as nestin, brain lipid binding protein (BLBP), vimentin, paired box gene 6 (Pax6) and SRY (sex-determining region Y)-box 2 (SOX2), which are commonly used markers for their identification[29]. In this work, the focus is set on SOX2 and vimentin, even though co-localization with BLBP and Pax6 was observed in separate experiments (data not shown).

SOX2 is a high-mobility group transcription factor, expressed in neuroectoderm, the earliest step in embryonic CNS development. It remains expressed in SVZ and SGZ of the adult brain, indicating the progenitor cells in the adult CNS. It has a critical role in maintaining proliferative and

undifferentiated state of progenitors, inhibiting the premature neuronal differentiation[29]. SOX2 is highly expressed in NEC and RGC, but is downregulated in neuron-specific progenitors. Precise control over SOX2 downregulation is crucial for transition from RGC to neurons[30]. SOX2 is also expressed in astrocytes and oligodendrocytes in embryonic and early postnatal development in rodents, but is downregulated in mature cells[31]. Importantly, it is a potent factor for reprogramming of glial cells into functional neurons in the adult CNS. *In vivo* research performed by Niu et al.[32] showed that the ectopic expression of SOX2 in mice is sufficient to reprogram astrocytes into induced adult endogenous progenitors generating neuroblasts. Neuroblasts were shown to be proliferative and generate mature neurons. Gu et al.[33] have shown that SOX2 expression is upregulated in rat hippocampus after TBI, indicating its role in the NPC mobilization in the early stages of TBI.

Two major intermediate filament proteins in astrocytes are vimentin and glial fibrillary acidic protein (GFAP). They provide mechanical support and structural plasticity due to their flexibility. Vimentin is expressed during early development in RGC, immature astrocytes, but also in fibroblasts and endothelial cells in CNS. Vimentin co-localizes with GFAP during the astrocyte maturation and differentiation and it may be necessary for GFAP formation and stabilization. In mature astrocytes, vimentin is downregulated, while GFAP remains expressed, making it a suitable marker for mature astrocyte identification and visualization. Both vimentin and GFAP are upregulated in CNS injury, suggesting their crucial role in astrogliosis and glial scar formation[34].

Immature neurons express cytoskeletal protein β-tubulin III, one of seven isotypes of β-tubulin, which alongside α-tubulins forms microtubules. Microtubules are involved in cell division, morphology maintenance and organelle transport. Five β-tubulin isotypes are expressed in mammalian brain. They are very conserved and vary in no more than 15 amino acids at

the carboxy-terminal protein region. β-tubulin III is the only phosphorylated tubulin and it differs about 10% in sequence from other β-tubulins expressed in brain. Commercial name of β-tubulin III, also used in this work, is TUJ1. TUJ1 is expressed during neuronal differentiation, serving as a newly-generated postmitotic neuron marker[35].

SRY-box transcription factor 9 (SOX9) belongs to the same transcription factor family as SOX2. SOX9 is expressed in RGC, astrocytes and oligodendrocyte progenitors in the embryonic and adult CNS. Its expression begins before RGC differentiation switch from neurons to glia, initiating the gliogenesis process during embryonic development of CNS[36]. Scott et al.[36] have found that SOX9 induces and maintains NPCs in the embryonic and in the adult CNS. In the absence of SOX9, astrocyte and oligodendrocyte progenitor number is reduced, while transient increase in neuroblasts was observed. Furthermore, SOX9 inhibits neuronal differentiation, and an increase in SOX9 expression diminishes neurogenesis. Kang et al.[37] have shown SOX9 controls induction of glial-specific genes by regulating the physiology of astrocyte progenitors during gliogenesis.

1.5. Opossum as a model for neuroregeneration studies

In this work, South American gray short-tailed opossum *Monodelphis domestica* is used. Unlike most marsupials, *M. domestica* lacks a pouch and the pups are born very immature. After 14 days of gestation, they proceed with development *ex utero*, clinging to the mother[38]. Therefore, they have extended period of postnatal development. Newborn pups are comparable to embryonic day (E)12 rats or E11.5 mice[39]. Developmental studies have shown that opossum cortical neurogenesis peaks between postnatal day (P)14 and P24. Gliogenesis begins at P18 with generation of astrocytes and it ends with generation of oligodendrocytes at P40 and later[40].

Opossums are used in neuroregenerative studies because they can fully regenerate the spinal cord after an injury during first two postnatal weeks[41]. As a result of the rostro-caudal gradient of development, spinal cord segments show different regeneration ability. Regeneration ability of opossums' spinal cord stops at P12 for the cervical part, and at P17 for less mature lumbar part[42]. Furthermore, in P4 opossums 1-2 weeks following the spinal cord injury, lesion place is closed as a result of regenerating and newly formed axons and it becomes functional[43]. In this research, P3-5 and P16-18 opossums (Figure 3) were used, because of their different capacity to regenerate spinal cord after injury.

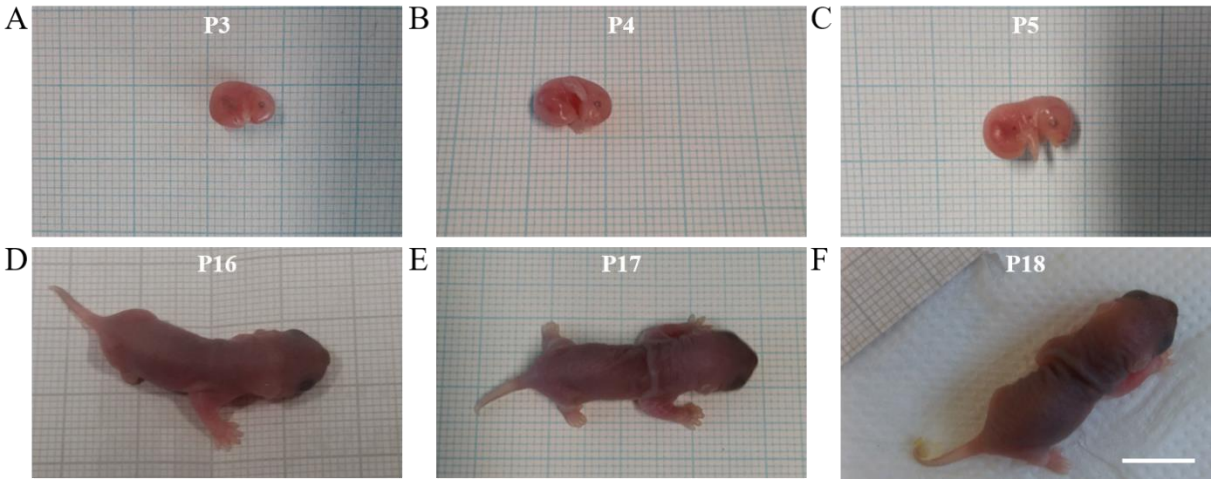

Figure 3 Monodelphis domestica *at postnatal ages used in this study. (A) P3, (B) P4, (C) P5, (D) P16, (E) P17, (F) P18 opossum pups. Scale bar, 1 cm.*

As a laboratory model, opossums provide several advantages. They can breed frequently throughout the year in captivity and are small and easy to maintain. The pups are easily accessible because of the absence of the pouch. Removal of opossum pups is done with zero harm to the mother and neonates can be accessible for experimental use at very immature stage.

2. Aim of the thesis

The main goal of this work was to establish and characterize a new *in vitro* neuronal culture derived from opossum *Monodelphis domestica*[44] that could provide additional mammalian model for the study of CNS regeneration.

This has been successfully obtained and described in our recent publication[44] (data not shown, but can be accessed online). The long-term primary cortical neuronal cultures from neonatal opossum can be maintained up until a month after the tissue collection. P3-5 opossum cortex give rise to almost pure neuronal culture with more than 93% of neurons. The cultures derived from P16-18 opossum cortex, have lower portion of neurons (around 80%), correlating to the gliogenesis initiation and increase in astrocyte number that reaches 20% after one week in culture.

The second aim of this thesis was to further characterize the cell composition using additional markers for both RGC and astrocytes. SOX2, SOX9 and vimentin were used and their expression was quantified in combination to GFAP or β-tubulin III.

Finally, the last aim was to develop a functional *in vitro* test including calcium imaging and scratch assay in order to assess the opossum cortex regeneration capacity. Cortex regeneration capacity is researched in two age groups, P3-5 and P16-18. By comparatively studying the CNS of opossums in developmentally different stages, the capacity of regeneration after the injury is observed, as well as the different permissiveness of the cell environment to the mechanism of regeneration.

We hypothesize that the expression of developmental markers, such as SOX2 and SOX9, in addition to vimentin and GFAP in the opossum primary neuronal cells would give an insight into molecules involved in promoting and inhibiting the cortical regeneration. Furthermore, we hypothesize that neurogenesis can be achieved in molecular environment which resembles to developmental conditions of the CNS.

3. Materials and methods

3.1. Animals

To obtain the primary neuronal cultures, South American gray short-tailed opossum (*Monodelphis domestica)* pups of both sexes at P3-5 and P16-18 were used. The opossum colony was maintained at the animal house facility of the University of Trieste, following the guidelines of the Italian Animal Welfare Act, and their use was approved by the Local Veterinary Service, the Ethics Committee board, and the National Ministry of Health (Permit Number: 1FF80.N.9Q3), following the European Union guidelines for animal care (d.1.116/92; 86/609/C.E.). The animals are housed in standard laboratory cages in a temperature- and humidity-controlled environment (27–28°C; 50–60% humidity) with a 12/12 h light/dark cycle and *ad libitum* access to food and water. All experiments described were performed in accordance with the European Directive 2010/63/EU for animal experiments. All efforts had been made to minimize the number of animals used and animal suffering.

3.2. Primary dissociated neuronal cultures

The dissociation protocol was developed following the established protocol for postnatal mice[45] with modifications described in Petrović et al.[44]. Schematic overview of the procedure is shown in Figure 4.

All the instruments were precleaned with 70% ethanol (Gram-mol, Zagreb, Croatia) and 1% Incidin (Ecolab, Zagreb, Croatia). 12 mm width coverslips (Thermo Fisher Scientific, Waltham, MA, USA) were washed in 1 M hydrochloric acid (Ru-Ve, Sv. Nedelja, Croatia) overnight at room temperature (RT, 20-22°C), following the wash with distilled water and absolute ethanol for an hour at RT. Coverslips were dried and spread in a glass Petri dish, then dry sterilized in the oven at 150°C for 90 minutes. Sterile coverslips were placed in wells of a 24-well tissue culture plate

(Sarstedt, Nümbrecht, Germany). Coverslips were coated with 150 µL of 50 µg/mL poly-L-ornithine (Sigma-Aldrich, St. Louis, Missouri, SAD) at 32°C overnight. The following day, poly-L-ornithine was removed from coverslips and coverslips were coated with 2 µg/mL laminin (Sigma-Aldrich). Primary neurons were isolated from the cortex of postnatal opossums of P3-5 and P16-18 age groups. Dissection was performed in the ice-cold oxygenated (95% O_2/5% CO_2) dissection solution (113 mM NaCl, 4.5 mM KCl, 1 mM $MgCl_2$ x $6H_2O$, 25 mM $NaHCO_3$, 1 mM NaH_2PO_4, 2 mM $CaCl_2$ x $2H_2O$, 11 mM glucose and 0.5% w/v Penicillin/Streptomycin/Amphotericin B, pH 7.4, all from Sigma–Aldrich, St. Louis, MO, USA). Both hemispheres were used, while olfactory bulbs, remaining subcortical structures and meninges were removed. The tissue was chopped into small pieces and washed three times with sterile phosphate-buffered saline (PBS) solution (137 mM NaCl, 2.7 mM KCl, 10 mM Na_2HPO4, 2 mM KH_2PO4, all from Sigma–Aldrich). Cortices were digested enzymatically with prewarmed trypsin in EDTA (Santa Cruz Biotechnology, SCBT, Dallas, TX, USA), incubating at thermo block set at 32.5°C. 0.5% w/v trypsin was used for P3-5 pups for 10 minutes, while 2.5% w/v trypsin was used for P16-18 pups for 15 minutes. Samples were washed three times in PBS and triturated in a trituration solution comprised of 10 mg/mL DNAse I (Sigma–Aldrich), 1 mg/mL trypsin inhibitor (SCBT), and 1% w/v bovine serum albumin (BSA; Pan-Biotech GmbH, Aidenbach, Germany) in Hank's Balanced Salt Solution (HBSS) solution, w/o Ca^{2+} and Mg^{2+} (Pan-Biotech). The tissues were triturated by mechanical pipetting using a 1 mL filter tip for at least 30 times to break the tissue structure. The supernatant was collected, and trituration was repeated two times for P3-5 and three times for P16-18 opossum pups. The supernatant with dissociated cells was layered on 5% w/v BSA in HBSS to remove the cell debris. Cells were centrifuged at 1000 rpm for 5 min at RT and resuspended in plating medium, consisting of Dulbecco's minimum essential medium (DMEM) with stable glutamine, supplemented with 10% w/v fetal bovine serum (FBS) and 1% w/v Penicillin/Streptomycin (all from Pan-Biotech).

The cells were preplated in the 35 mm Petri dish (Sarstedt) and incubated at 32°C for 5 minutes to remove fibroblasts. Cells were counted using the hemocytometer and the cell solution was diluted in 15 mL tubes (Carl Roth, Karlsruhe, Germany) in the plating medium at the density of 1 x 10^4 cells per well. The next day, 2/3 of the plating medium was replaced with neuronal medium containing Neurobasal medium, supplemented with B27 (both from Thermo Fisher Scientific), 1 mM L-glutamine and 1% Penicillin/Streptomycin (both from Pan-Biotech). The neuronal primary cultures were maintained in an incubator at 32ºC with 5% CO_2 and 95% relative humidity. Subsequent media changes were done once weekly, changing only a half of the medium with fresh prewarmed neuronal medium.

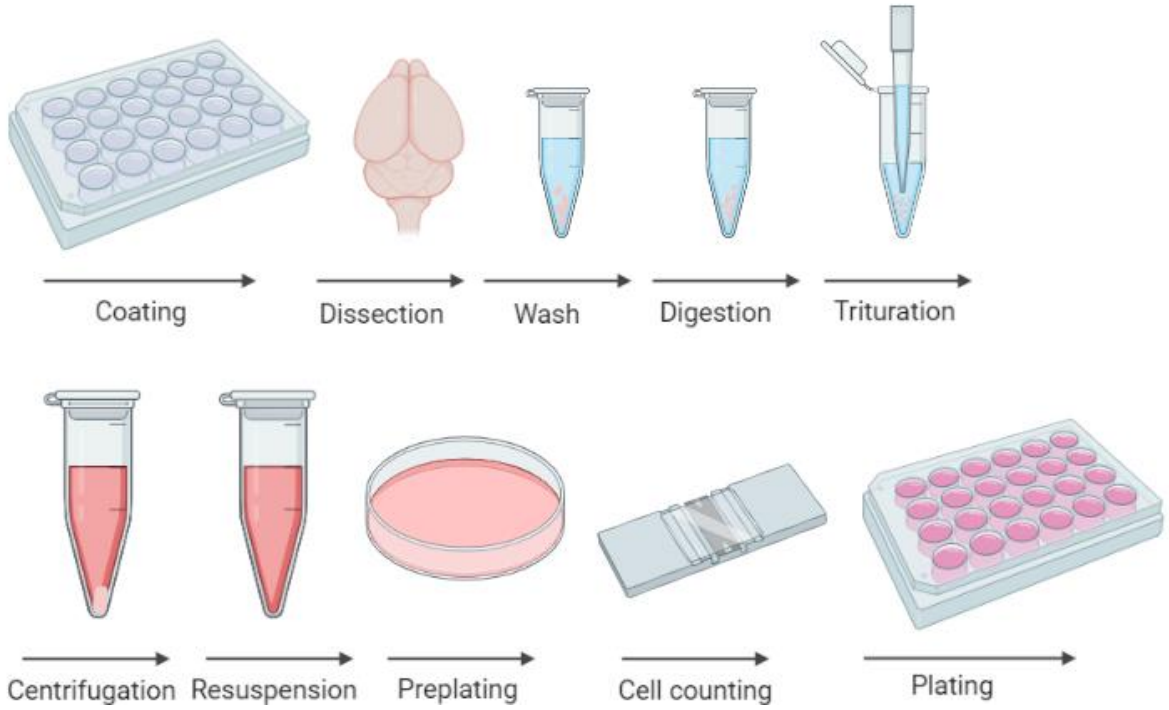

Figure 4 Schematic overview of obtaining the primary cell cultures. Illustration was created with BioRender.com.

3.3. Neuroregeneration scratch assay

The cells were plated at the density of 1 x 10^4 cells per well in a 24-well plate on 12 mm width glass coverslips, as described previously. The neuronal primary cultures were maintained in an incubator at 32ºC with 5% CO_2 and 95% relative humidity. Subsequent media changes were done once weekly, changing a half of the medium with fresh prewarmed neuronal medium. On DIV7, DIV10 and DIV14, a scratch assay was performed in the middle of the coverslip, damaging the cells with 0.1 mm tip tweezers, causing a scratch approximately 100 µm wide. Cells were either fixed with 4% paraformaldehyde (PFA, Sigma–Aldrich) with 200 mM sucrose (Sigma-Aldrich) in PBS, pH 6.9, 24 or 48 hours after the scratch assay and immunostained; or examined for calcium activity 24, 48 and 72 hours after the scratch assay.

3.4. Immunofluorescence

3.4.1.Immunocytochemistry

Cells were removed from the neuronal medium and fixed for 20 minutes at RT with 4% PFA (Sigma–Aldrich) with 200 mM sucrose (Sigma-Aldrich) in PBS, pH 6.9. Following the fixation, cells had been washed three times with PBS, saturated with 0.1 M glycine (Sigma-Aldrich) and washed again with PBS, each step for 5 minutes. 0.1% Triton X-100 (Sigma-Aldrich) in PBS was used to permeabilize cell membranes for 10 minutes, then washed with PBS for 5 minutes. Blocking was performed with 0.5% w/v BSA (Pan-Biotech) in PBS for 30 min. Then the cells were transferred in dark, humid chamber and incubated with primary antibodies for one hour. 100 µL od antibody solution was dropped onto the coverslip. After the primary antibody incubation, cells were washed in PBS twice for 5 minutes, then proceeded with secondary antibody and cell nuclei stain incubation for 30 minutes. After the incubation, coverslips were washed two times with PBS and once with dH_2O for 5 minutes. Microscope slides (Thermo Fisher

Scientific, Waltham, MA, USA) were precleaned with 70% ethanol and dried, then a drop of mounting medium (Vectashield, Vector Laboratories, Burlingame, CA, USA) was added to the slides. Coverslips were mounted face-down on the mounting medium and sealed with nail polish. Slides were left to dry in the dark for an hour at RT and stored at 4°C upon the analysis using the fluorescent microscope. All the incubations and washing steps were performed at RT.

0.5% w/v BSA (Pan-Biotech) in PBS was used to dilute the primary and secondary antibodies, while the cell nuclei were stained with 300 nM nuclear stain 4’,6-diamidino-2-phenylindole (DAPI, Thermo Fisher Scientific) in 0.5% w/v BSA (Pan-Biotech) in PBS. F-actin staining was performed with Phalloidin-iFluor 488 (Abcam, Cambridge, UK) at 1:500 dilution in 0.5% w/v BSA (Pan-Biotech) in PBS and incubated for 30 min alongside with the secondary antibodies and the cell nuclei stain. Primary antibodies used in this thesis are listed in Table 1, while secondary antibodies are listed in Table 2.

Table 1 Primary antibodies used in this work.

Primary antibody	Host and type	Dilution	Immunogen	Producer Cat # RRID
Anti - SOX2 antibody [9-9-3]	Mouse monoclonal IgG1	1:200	Synthetic peptide conjugated to KLH derived from within residues 300 to the C-terminus of Human SOX2.	Abcam, Cat# ab79351, RRID: AB_10710406
Anti - SOX9 antibody [EPR14335-78]	Rabbit monoclonal IgG	1:300	Recombinant fragment within Human SOX9 aa 150-300 (internal sequence).	Abcam, Cat# ab185966, RRID: AB_2728660
Anti-Tubulin β 3 (TUBB3) Antibody (TUJ1)	Mouse monoclonal IgG2a	1:200	Microtubules derived from rat brain.	Biolegend, Cat# 801201, RRID: AB_10063408
Anti - Vimentin antibody [EPR3776]	Rabbit monoclonal IgG	1:400	Synthetic peptide within Human Vimentin aa 400 to the C-terminus (C terminal). The exact sequence is proprietary.	Abcam, Cat# ab92547, RRID: AB_10562134
Anti - Vimentin antibody	Mouse monoclonal IgG1	1:400	Aa 350-500. Purified vimentin from pig eye lens.	Abcam, Cat# ab8069, RRID: AB_306239
Anti – GFAP antibody	Mouse monoclonal IgG1	1:300	GFAP from pig spinal cord.	Sigma-Aldrich, Cat# G3893, RRID: AB_477010

Table 2 Secondary antibodies used in this work.

Secondary antibody	Host and type	Dilution	Immunogen	Producer Cat # RRID	Conjuga-tion
Goat anti-mouse IgG (H+L)	Goat polyclonal IgG	1:400	Gamma Immunoglobins Heavy and Light chains	Thermo Fisher Scientific, Cat# A32723, RRID: AB_2633275	Alexa Fluor® 488
Goat anti-mouse IgG (H+L)	Goat polyclonal IgG	1:400	Not available	Abcam, Cat# ab150118, RRID: AB_2714033	Alexa Fluor® 555
Goat anti-mouse IgG1	Goat polyclonal IgG1	1:300	IgG gamma 1	Thermo Fisher Scientific, Cat# A21121, RRID: AB_2535764	Alexa Fluor® 488
Goat anti-mouse IgG2a	Goat polyclonal IgG2a	1:300	Mouse IgG2a	Thermo Fisher Scientific, Cat# A21137, RRID: AB_2535776	Alexa Fluor® 555
Goat anti-rabbit IgG (H+L)	Goat polyclonal IgG	1:400	Gamma Immunoglobins Heavy and Light chains	Thermo Fisher Scientific, Cat# A32731, RRID: AB_2633280	Alexa Fluor® 488
Goat anti-rabbit IgG (H+L)	Goat polyclonal IgG	1:400	Gamma Immunoglobins Heavy and Light chains	Thermo Fisher Scientific, Cat# A32732, RRID: AB_2633281	Alexa Fluor® 555
Goat anti-rabbit IgG (H+L)	Goat polyclonal IgG	1:300	Not available	Abcam, Cat# ab150083, RRID: AB_2714032	Alexa Fluor® 647

3.4.2. Calcium imaging

The cells were plated at the density of 1 x 10^4 cells per well in 24-well tissue culture plate (Sarstedt, Nümbrecht, Germany) as described previously. Cells were incubated at 32ºC with 5% CO_2 and 95% relative humidity. Subsequent media changes were done once weekly, changing a half of the medium with fresh prewarmed neuronal medium. At desired time point after the plating or scratch assay, cells were transferred to a 35 mm, high µ-Dish 35 mm (Ibidi, Gräfelfing, Germany). Cells were loaded with a cell-permeable calcium dye Fluo-4 AM (Abcam, Cat# ab241082) by incubating them with 4 µM Fluo-4 AM dissolved in DMSO (Carl Roth, Cat# 4720.4, stock solution 4 mM) and Pluronic F-127 20% solution in DMSO (Thermo Fisher Scientific, Cat# P3000MP) at a ratio of 1:1 in prewarmed Ringer's solution (145 mM NaCl, 3 mM KCl, 1.5 mM $CaCl_2$, 1 mM $MgCl_2$, 10 mM glucose and 10 mM HEPES, pH 7.4) at 32°C for 1 hour. After incubation, cultures were washed with Ringer's solution and incubated for 15 min twice at 32°C to allow complete intracellular de-esterification of the dye and then transferred to the stage of Olympus IX83 (Olympus, Tokyo, Japan) inverted fluorescent microscope.

3.5. Fluorescence microscopy

Cell samples were analyzed using an Olympus IX83 inverted fluorescent microscope (Olympus) equipped with differential interference contrast (DIC) and fluorescence optics mirror units (Table 3). Fluorescence images were obtained with Hamamatsu Orca R2 CCD camera (Hamamatsu Photonics, Hamamatsu, Japan) and CellSens software (Olympus). Objectives used were 10x/0.3 numerical aperture (NA) air, 20x/0.5 NA air; and 40x/1.4 NA and 60x/1.42 NA with oil immersion.

For each immunocytochemistry sample, minimum of 10 frames were obtained at slice spacing of 2 µm for 10x, 1.27 µm for 20x, 0.35 µm for 40x and 0.24 µm for 60x objective. Maximum intensity projection was used for

each image. Image processing and analysis were performed with CellSens software and ImageJ/FIJI by W. Rasband (developed at the U.S. National Institutes of Health).

Table 3 Filter cube set used for fluorescence microscopy (Chroma, Irvine, CA, USA).

	Unit Name	**Excitation filter**	**Emission filter**	**Dichromatic mirror**
Ultraviolet Excitations	U-FUNA	360-370	420-460	410
Blue Excitations	U-FBW	460-495	510IF	505
Green Excitations	U-FGW	530-550	575IF	570
Far-Red Excitations	Cy5	590-650	663-738	660

For calcium imaging, top stage incubator with temperature controller unit (Ibidi, Gräfelfing, Germany) were added onto the microscope. The temperature was set constant to 32.5°C throughout the experiment, which was conducted in Ringer's solution. Movies were acquired with 10x/0.3NA and 20x/0.5 NA objective at a sampling rate of 3–10 Hz with a spatial resolution of 1344 x 1024 pixels for 5-15 minutes. To avoid saturation of the signals, excitation light intensity was attenuated by 25ND25 and 50ND50 neutral density (ND) filters (Olympus). Movie processing and analysis were performed with CellSens software and ImageJ by W. Rasband (developed at the U.S. National Institutes of Health).

3.6. Data analysis

Statistical analysis was performed using the GraphPad Prism 8.4 software (GraphPad Software Inc., San Diego, California, USA). To calculate the normality of data distribution, D'Agostino-Pearson or Shapiro-Wilk normality test was used. Brown-Forsythe test was used to test the assumption that all data are sampled from populations with the same standard deviations.

Three or more data groups were compared using one-way ANOVA, based on the assumption that the populations are Gaussian and that the variances are equal. Following one-way ANOVA parametric test, the post hoc Holm-Šídák test was used for multiple comparisons between the two data groups. Data groups with different variances that fail a normality test were compared using the Kruskal-Wallis test. Following Kruskal-Wallis nonparametric test and post hoc Dunn's multiple comparisons test. Data groups with equal variances that follow Gaussian distribution were compared using the Welch's ANOVA and post hoc Dunnett's T3 multiple comparisons test.

The p value was adjusted for multiple comparisons. For comparison of two normally distributed data groups, unpaired t test was used. The t test assumption that the two samples come from populations with identical standard deviations was tested using the F test. In case of unequal variances, the Welch's t test was used.

The accepted level of significance was $p < 0.05$. Decimal format used to report p values follows the recommended NEJM (New England Journal of Medicine) style (Table 4).

Table 4 New England Journal of Medicine defined accepted levels of statistical significance.

p value	Wording	Summary
< 0.001	Very significant	***
0.001 – 0.01	Very significant	**
0.01 – 0.05	Significant	*
≥ 0.05	Not significant	Ns

For analysis of calcium imaging experiments, intensity of each selected region of interest (ROI) was obtained at every frame. ROI parameters were set to fully fit inside the soma of cells and fixed for every ROI. Data was analyzed by Microsoft Excel (Microsoft, Redmond, Washington, SAD) and GraphPad prism 8.4 software (GraphPad Software Inc.). Minimum of intensity (F_0) was obtained for every ROI and an average of six values within the minimal intensity were calculated. A ratio of change in fluorescence intensity ($\Delta F/dF$) with minimum of intensity were calculated. Values were analyzed and time-lapse graphical representations were obtained in GraphPad Prism 8.4.

4. Results

4.1. Establishment of primary cell cultures

We have recently published detailed protocol for the establishment of primary neuronal cultures from neonatal *Monodelphis domestica*[44]. Some of the presented results are referred to the mentioned article, however additional findings and characterization have been made and are described in this thesis.

Primary cortical dissociated cultures were obtained from P3-5 and P16-18 opossums. Cultures survived well maintained at 32ºC with 5% CO_2 and 95% relative humidity for more than a month for P3-5 opossums and up to 3 weeks for P16-18 opossums. Dissociation of P16-18 cortex was more difficult to perform and those cultures had lower survival and an increased number in non-neuronal cells, as expected[45].

4.2. Maturation of primary cell cultures using immunocytochemistry *in vitro*

One day after cell plating, neurons formed first neurites that later developed into axons and dendrites. Neuronal GCs, formed at the tips of neurites were stained with TUJ1 and phalloidin (Figure 5A, B, arrows indicating GCs). Neurons continued to grow their processes and became arborized after few days in culture. As published, for P3-5 cultures, the percentage of TUJ1-positive neurons was highest at DIV4, when it reached 92.66 ± 2.02%, n = 603. Between DIV4 and DIV7, instead of GCs, first neuronal connections are evident, while actin filaments indicate the formation of dendritic spines (Figure 5C, D). TUJ1-positive cell number decreased (86.28 ± 4.25%, n = 980), while GFAP-positive cells increased (5.71 ± 0.53%, n = 1,948). For P16-18 cultures, lower portion of cells were positive for TUJ1 at DIV1 (72.80 ± 4.67%, n=2,070), compared to P3-5 cultures. At DIV7, TUJ1-positive cells increased to 82.37 ± 3.67%, n=704, while GFAP positive cells consisted of 19.35 ± 0.83% (n=1,085)[44].

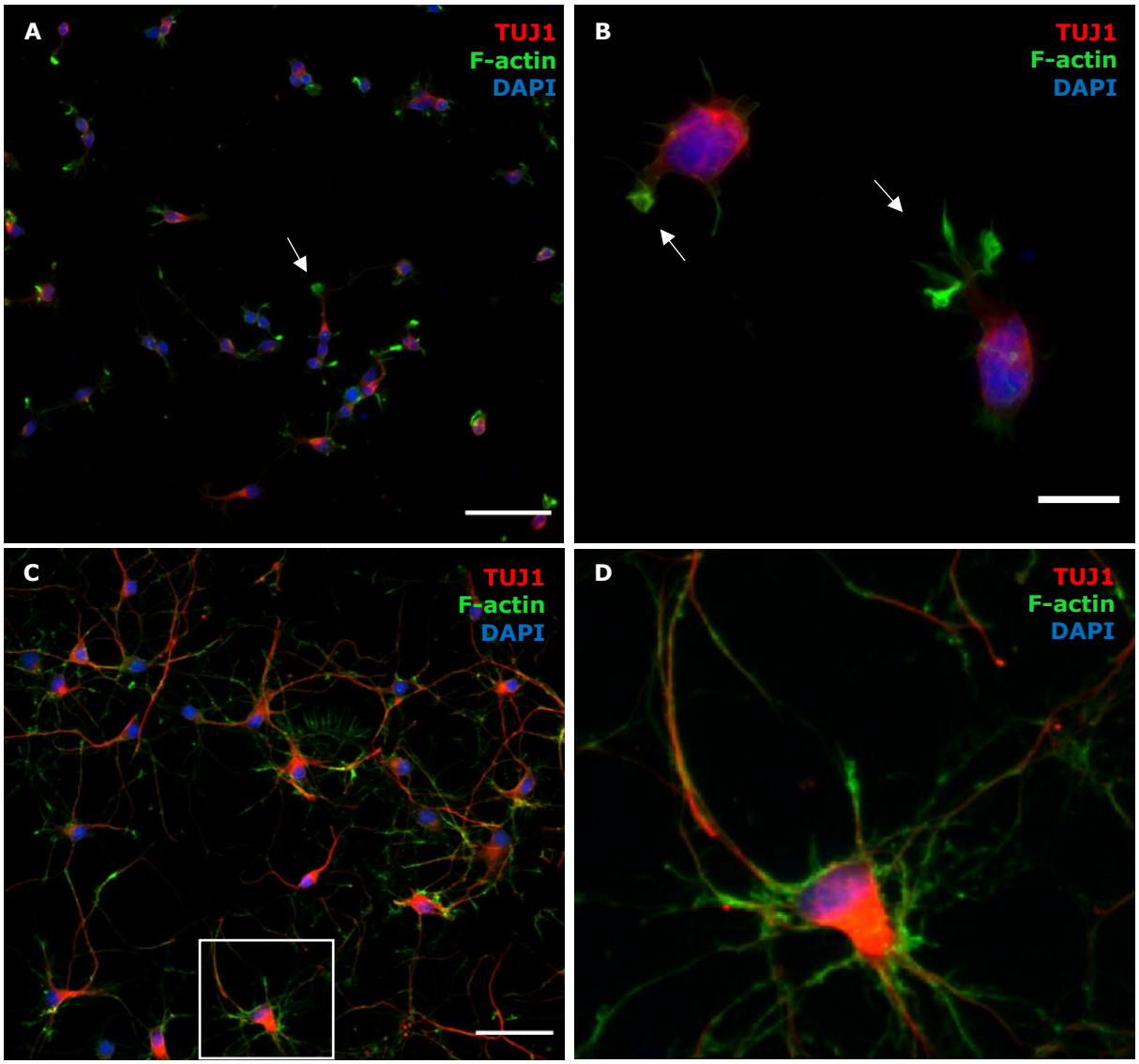

Figure 5 Primary neuronal cultures derived from P3-5 opossum pups stained for β-tubulin III (TUJ1, red), filamentous (F)-actin (green) and nuclear stain (DAPI, blue). Cultures were fixed and stained at (A) DIV1, scale bar, 50 µm. Arrow is pointing to a GC; (B) DIV1, scale bar 10 µm. Arrow is pointing to a GC; (C) DIV7, scale bar 50 µm. (D) Enlarged inset from (C) image.

At DIV7, neurons in both P3-5 and P16-18 formed connections (Figure 6). Neuronal morphology becomes complex with elaborate processes and long axons extending to nearby cells. Each neuron has multiple dendrites and more fine processes surrounding the soma. Astrocytes became more evident at DIV7 and, in addition to GFAP, express vimentin.

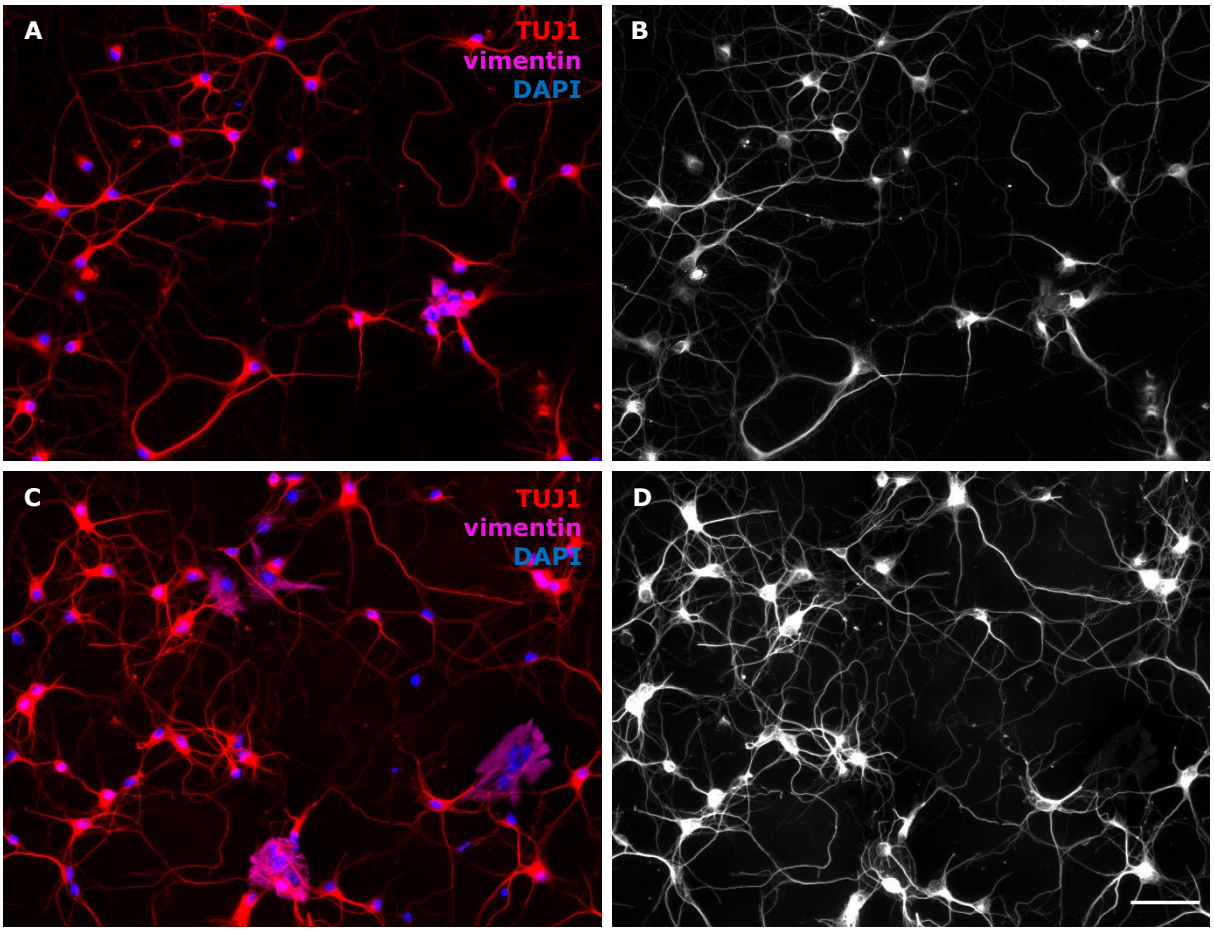

Figure 6 Expression of immature neuronal marker (βIII-tubulin, TUJ1, red), immature astrocyte marker (vimentin, magenta) and nuclei (DAPI, blue) at DIV7 primary neuronal cultures. Cells were obtained from (A, B) P3-5 opossum and (C, D) P16-18 opossum pups, respectively. For better visualization, grayscale images of TUJ1 are shown (B, D). Scale bar, 50 µm.

In vitro maturation of primary cell cultures was monitored by expression of SOX2 (Table 5) and SOX9 (Table 6). At DIV7, SOX2 is expressed in 45.21 ± 10.78% cells (n=424) in P3-5 cultures (Figure 7A, C, D) and in P16-18 cultures in 31.00 ± 3.66% cells (n=379, Figure 7B, E, F). Its expression stays virtually unchanged at DIV11 and decreases at DIV16 in P3-5 cultures. In contrast, SOX2 expression decreases in DIV10 and remains almost unchanged in DIV14 of P16-18 cultures.

Table 5 SOX2 expression and co-expression with TUJ1 in P3-5 and P16-18 cortical-derived opossum cultures at various days in vitro. Values are expressed as mean ± standard deviation.

		SOX2	$SOX2^+TUJ1^-$	$SOX2^+TUJ1^+$	Cells analyzed
P3-5	DIV7	45.21 ± 10.78%	14.81 ± 12.14%	30.30 ± 21.38%	424
	DIV11	47.66 ± 5.04%	14.57 ± 4.39%	32.93 ± 5.33%	422
	DIV16	34.70 ± 17.84%	9.99 ± 5.55%	25.33 ± 12.82%	457
P16-18	DIV7	31.00 ± 3.66%	26.27 ± 6.62%	3.17 ± 3.45%	379
	DIV10	26.36 ± 10.92%	23.33 ± 11.49%	3.31 ± 3.28%	620
	DIV14	26.63 ± 8.96%	18.25 ± 10.11%	8.66 ± 2.15%	274

Interestingly, SOX2 and TUJ1 co-expression was observed (Table 5, Figure 7A, B). Double positive $SOX2^+TUJ1^+$ cells could be neuron-specific progenitor cells or immature neurons that retain SOX2 expression[30,32]. $SOX2^+TUJ1^+$ cells are present in 30.30 ± 21.38% of cells (n=424) in P3-5 cultures. However, in P16-18 cultures, $SOX2^+TUJ1^+$ cells are present in only 3.17 ± 3.45% of cells (n=379). Proportion of $SOX2^+TUJ1^+$ cells decrease in DIV16 of P3-5 cultures, while in P16-18 cultures, the proportion increases in DIV14.

$SOX2^+TUJ1^-$ are likely to be progenitor cells that could differentiate into both neurons and glia[46]. In P3-5 cultures, they represent 14.81 ± 12.14% of cells (n=424); and in P16-18 cultures, they account for 26.27 ± 6.62% of cells at DIV7 (Table 5). $SOX2^+TUJ1^-$ expression decreases in both age groups around the second week *in vitro*.

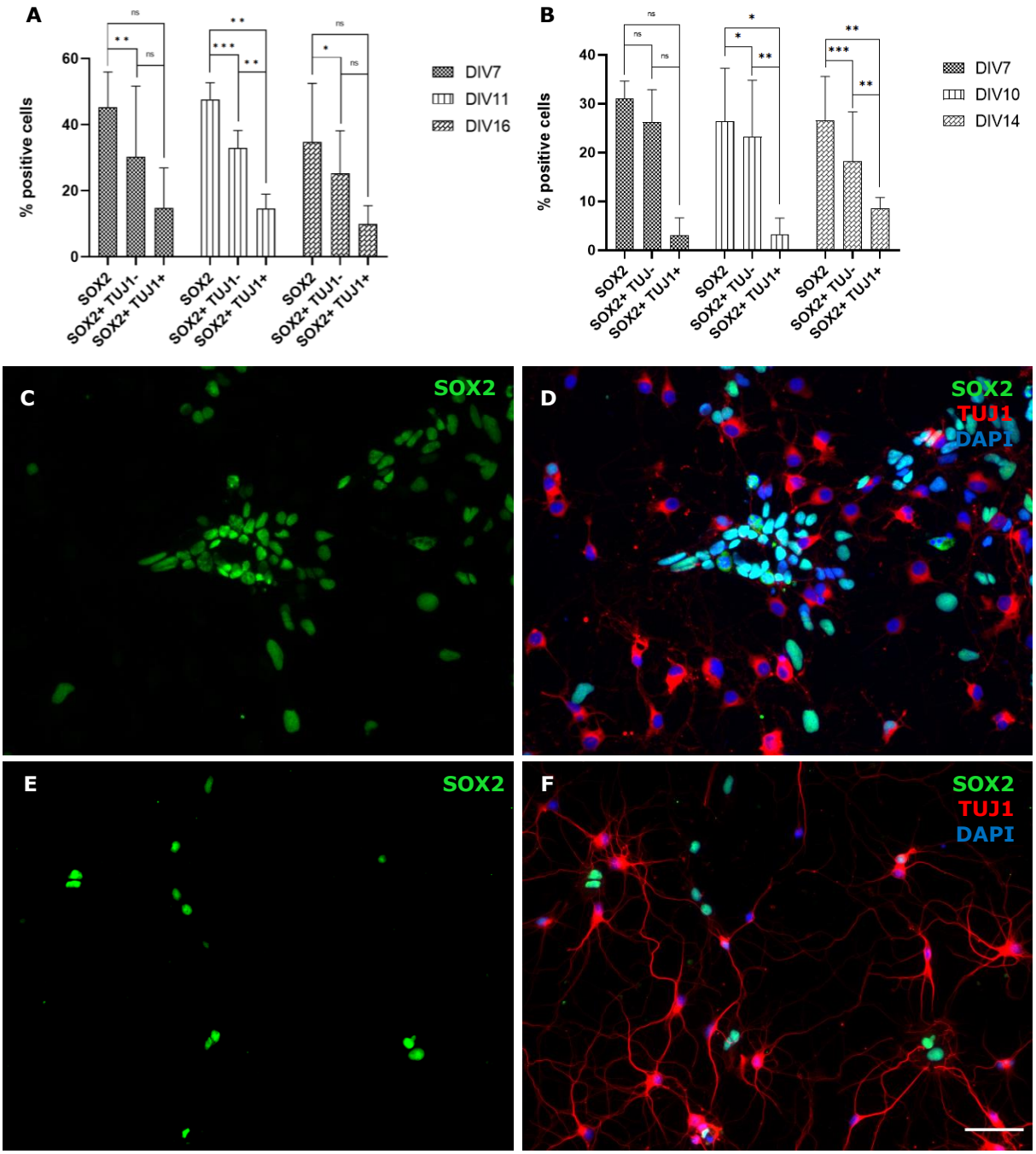

*Figure 7 Expression of SOX2 in P3-5 and P16-18 opossum cultures. Histogram showing the percentage of SOX2 expression and co-expression with βIII-tubulin (TUJ1) at different time points of in vitro maturation for (A) P3-5 and (B) P16-18 cultures. (A) One-way ANOVA followed by Holm–Šídák multiple comparisons test for DIV7, DIV11 and DIV16. SOX2 vs. $SOX2^{+}TUJ1^{-}$ p=0.005** in DIV7, p<0.001*** in DIV11 and p=0.03* in DIV16. SOX2 vs. $SOX2^{+}TUJ1^{+}$ $p=0.20^{ns}$ in DIV7, p=0.006** in DIV11 and $p=0.51^{ns}$ in DIV16. $SOX2^{+}TUJ1^{-}$ vs. $SOX2^{+}TUJ1^{+}$ $p=0.18^{ns}$ in DIV7, p=0.001** in DIV11 and $p=0.19^{ns}$ in DIV16. (B) Kruskal-Wallis test followed with Dunn's multiple comparisons test for DIV7. One-way ANOVA followed by Holm–Šídák multiple comparisons test for DIV10 and DIV14. SOX2 vs. $SOX2^{+}TUJ1^{-}$ $p>0.99^{ns}$ in DIV7, p=0.04* in DIV10 and p<0.001*** in DIV14. SOX2 vs. $SOX2^{+}TUJ1^{+}$ $p=0.08^{ns}$ in DIV7, p=0.02* in DIV10 and p=0.08** in DIV14. $SOX2^{+}TUJ1^{-}$ vs. $SOX2^{+}TUJ1^{+}$ $p=0.47^{ns}$ in DIV7, p=0.002** in DIV10 and p=0.008** in DIV14. SOX2 (green) cell co-expression with TUJ1 (red) with nuclear stain DAPI (blue) at DIV7 in (C, D) P3-5 cultures and (E, F) P16-18 opossum cultures. Scale bar, 50 μm.*

SOX9 is expressed in 16.29 ± 12.18% (n=441) of cells in P3-5 cultures at DIV7 (Figure 8A, C, D, Table 6). Its expression at DIV7 of P16-18 cultures is higher in 22.31 ± 13.21% of cells (n=224, Figure 8B, E, F). SOX9 expression rises in P3-5 cultures during cultivation *in vitro*, reaching 30.81 ± 14.67% of cells (n=395) at DIV16. In contrast, SOX9 expression in P16-18 samples decreases in DIV10 and increases in DIV14 cultures.

Table 6 SOX9 expression and co-expression with vimentin in P3-5 and P16-18 cortical-derived opossum cultures at various days in vitro. Values are expressed as mean ± standard deviation.

		SOX9	**SOX9$^+$vim$^+$**	**SOX9$^+$vim$^-$**	**Cells analyzed**
P3-5	**DIV7**	16.29 ± 12.18%	16.29 ± 12.18%	0.00 ± 0.00%	441
	DIV11	26.64 ± 1.96%	26.43 ± 1.81%	0.21 ± 0.47%	473
	DIV16	30.81 ± 14.67%	30.17 ± 14.13%	0.64 ± 0.61%	395
P16-18	**DIV7**	22.31 ± 13.21%	21.26 ± 13.78%	1.50 ± 2.47%	224
	DIV10	14.08 ± 7.92%	12.86 ± 6.95%	1.22 ± 2.05%	574
	DIV14	18.82 ± 14.61%	18.82 ± 14.61%	0.00 ± 0.00%	326

SOX9 co-expression is observed with vimentin (Table 6, Figure 8A, B). Almost every SOX9-positive cell is also positive for vimentin in both P3-5 and P16-18 cultures at every time point. These SOX9$^+$vim$^+$ cells appear to be the RGCs, which switched from generation of neurons into astrocytes[36]. Only a small portion of cells in P3-5 and P16-18 cultures is SOX9$^+$vim$^-$. SOX9$^+$vim$^-$ cells slightly increase in P3-5 cultures, but do not exceed 1% of the cells in DIV16. In P16-18 cultures, SOX9$^+$vim$^-$ cells decrease from around 1.5% in DIV7 to 0% of cells in DIV14.

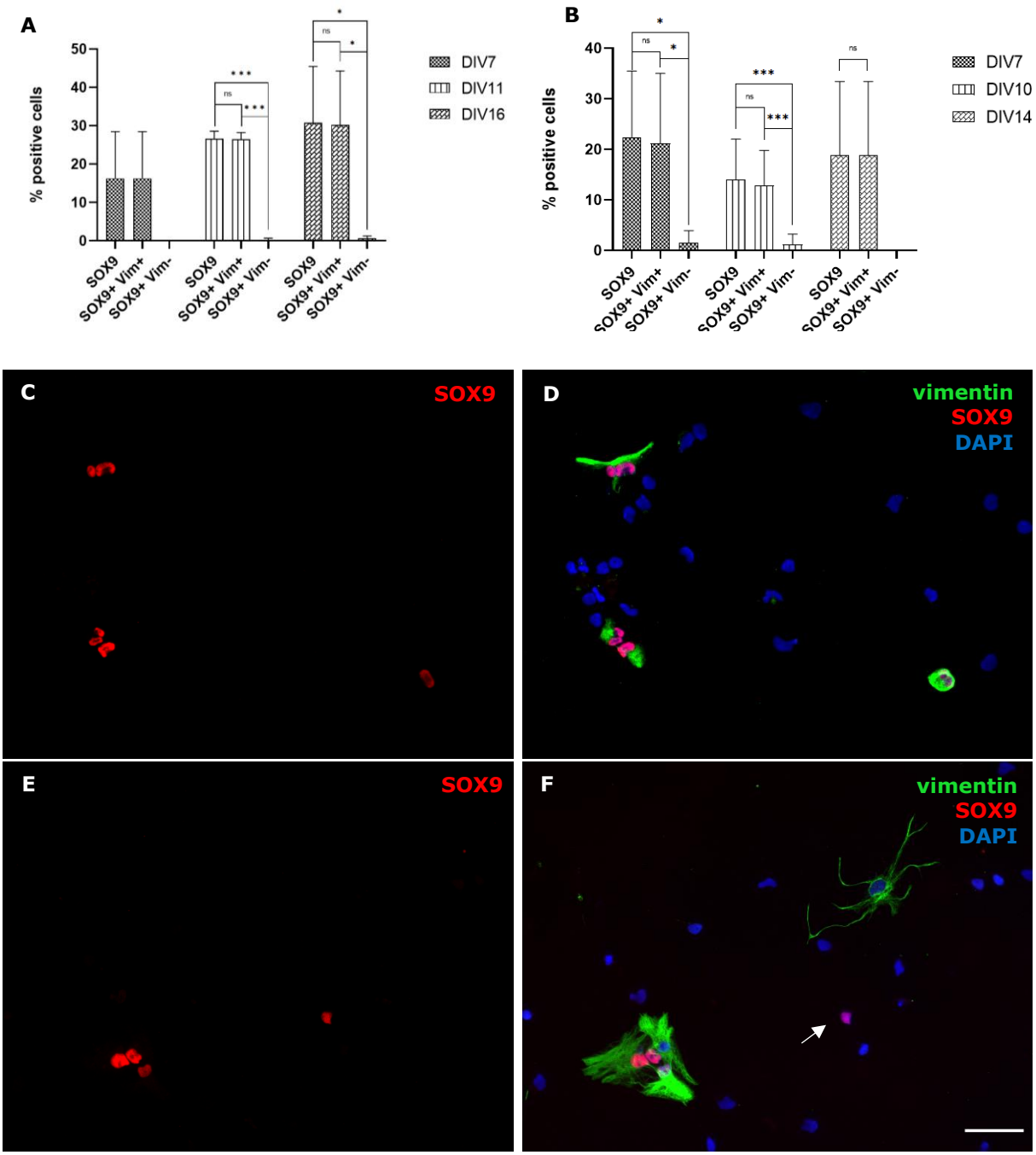

*Figure 8 Expression of SOX9 in P3-5 and P16-18 opossum cultures. Histogram showing the change of expression of SOX9, double positive SOX9^{+}vim^{+} and SOX9viim^{-} cells at different time points of in vitro maturation for (A) P3-5 and (B) P16-18 opossum cultures. (A) One-way ANOVA followed by Holm–Šídák multiple comparisons test for DIV11 and DIV16. SOX9 vs. SOX9^{+}vim^{+} p=0.98^{ns} for DIV11, p>0.99^{ns} for DIV16, SOX9 vs. SOX9^{+}vim^{-} p<0.001*** for DIV11, p=0.05* for DIV16. SOX9^{+}vim^{+} vs. SOX9^{+}vim^{-} p<0.001*** for DIV11 and p=0.05* for DIV16. (B) One-way ANOVA followed by Holm–Šídák multiple comparisons test for DIV7 and DIV14. Brown-Forsythe and Welch ANOVA tests of DIV10 followed with Dunnett's T3 multiple comparisons test. SOX9 vs. SOX9^{+}vim^{+} p>0.99^{ns} in DIV7, DIV10 and DIV14. SOX9 vs. SOX9^{+}vim^{-} p=0.01* in DIV7, p<0.001*** in DIV10, p=0.14^{ns} in DIV14. SOX9^{+}vim^{+} vs. SOX9^{+}vim^{-} p=0.02* in DIV7 and p<0.001*** in DIV10. SOX9 (red) cell co-expression with vimentin (green) with nuclear stain DAPI (blue) at DIV7 in (C, D) P3-5 cultures and (E, F) P16-18 opossum cultures. Arrow is pointing to SOX9^{+}vim^{-} cell. Scale bar, 50 µm.*

To further characterize the maturation of opossum-derived cortical astrocytes, a comparison between GFAP and vimentin expression was performed at DIV7 for both P3-5 and P16-18 samples.

Both P3-5 and P16-18 cultures consisted of stellate and protoplasmic astrocytes, but in general, protoplasmic astrocytes were more common. In P3-5 cultures astrocytes were less mature with thinner, less elaborated processes, indicating their immature state (Figure 9B). Higher number of cells that expressed vimentin than GFAP was observed. 22.20 ± 11.29% cells expressed vimentin and 12.72 ± 6.70% cells expressed GFAP in P3-5 cultures (n=352). Every $GFAP^+$ cell also co-expressed vimentin (Figure 9A). In P16-18 age group cultures, astrocytes had more complex and elaborated morphology (Figure 9C, D). 31.69 ± 10.98% of cells were vim^+ and 26.87 ± 13.07% cells were $GFAP^+$. (n=398) In contrast to P3-5 cortical cultures, not every $GFAP^+$ cell was vim^+ (inset in Figure 9D), confirming that *in vitro* maturation of astrocytes proceeds with vimentin downregulation. 21.68 ± 10.98% were $GFAP^+vim^+$ cells (Figure 9A).

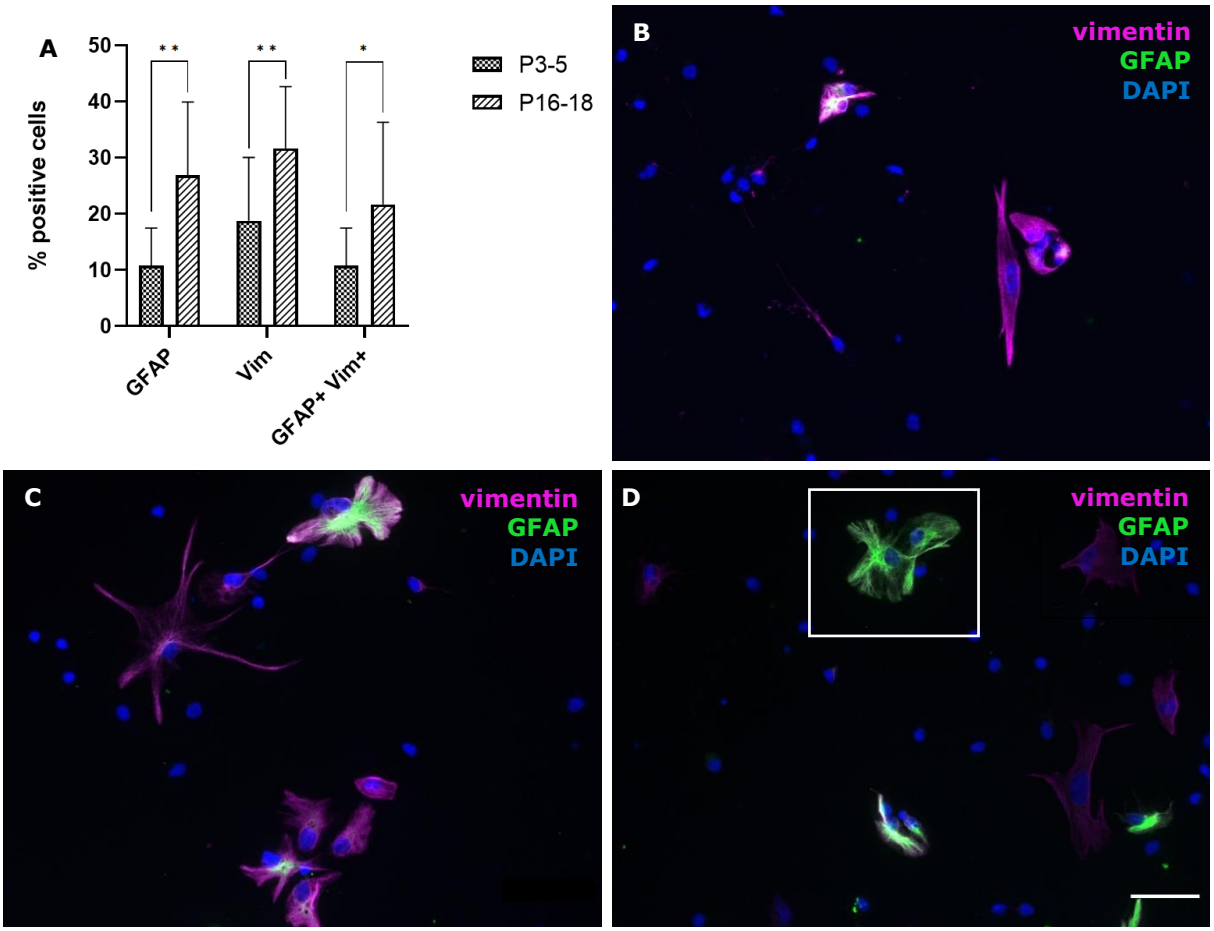

*Figure 9 Glial cells in primary cultures from P3-5 and P16-P18 opossum pups at DIV7. (A) Histogram showing the percentage of GFAP⁻ and vim⁺ cells among total number of analyzed cells for each age group, respectively. Welch's unpaired t test for GFAP and GFAP⁺vim⁺ comparison, unpaired t test for vimentin comparison. GFAP P3-5 vs. P16-18 p=0.002**, vim P3-5 vs. P16-18 p=0.01**, GFAP⁺vim⁺ P3-5 vs. P16-18 p=0.04*. Astrocytes were stained at DIV7 with vimentin (magenta), GFAP (green) and nuclei with DAPI (blue) for (B) P3-5 opossum cultures, (C, D) P16-18 opossum cultures. Inset in (D) shows an example of GFAP⁺vim⁻ astrocyte. Scale bar, 50 µm.*

4.2.1. Functional maturation of primary cell cultures *in vitro*

The functional maturation of *M. domestica* primary cell cultures was examined with calcium imaging method. Spontaneous calcium activity was observed in neurons in form of bursts of action potentials, as well as propagation of calcium waves in and between astrocytes (data not shown), confirming the formation of functional cell networks. Moreover, coordinated activity between astrocytes and surrounding neurons was observed as well. In this thesis, calcium imaging preliminary results are shown, considering that, to the best of our knowledge, these experiments have not yet been performed on *M. domestica* primary neuronal cultures. Therefore, the setting and optimization of the calcium imaging protocol encounted for a significant part of this work.

4.2.1.1. Establishment of calcium imaging method on M. domestica primary cell cultures

Cells were plated at the density of 1 x 10^4 cells per well in 24-well tissue culture plate and first experiments were performed at DIV7, when cells formed networks. Cell-permeable calcium indicator Fluo-4 AM was used alongside non-ionic copolymer surfactant Pluronic F-127 suitable for use in living cells. Pluronic F-127 solubilizes hydrophobic dye molecules and facilitates the cell loading of Fluo-4 AM dye. Calcium loading followed with washing steps has stained cells in the sample (Figure 10). Calcium indicator allows visualization of neuronal cell bodies, axons and thicker neurites. It also stains astrocytes (inset in Figure 10A). Protoplasmic astrocytes can be easily identified, while stellate astrocytes require careful observation in order to be distinguished from neurons. At DIV7 or at later time points, neurons develop a long axon that can be visualized by calcium indicator, and also, they have smaller nuclei than astrocytes. Moreover, dying cells can be visualized with higher dye intensity, because Ca^{2+} overload is commonly observed during cell death[47].

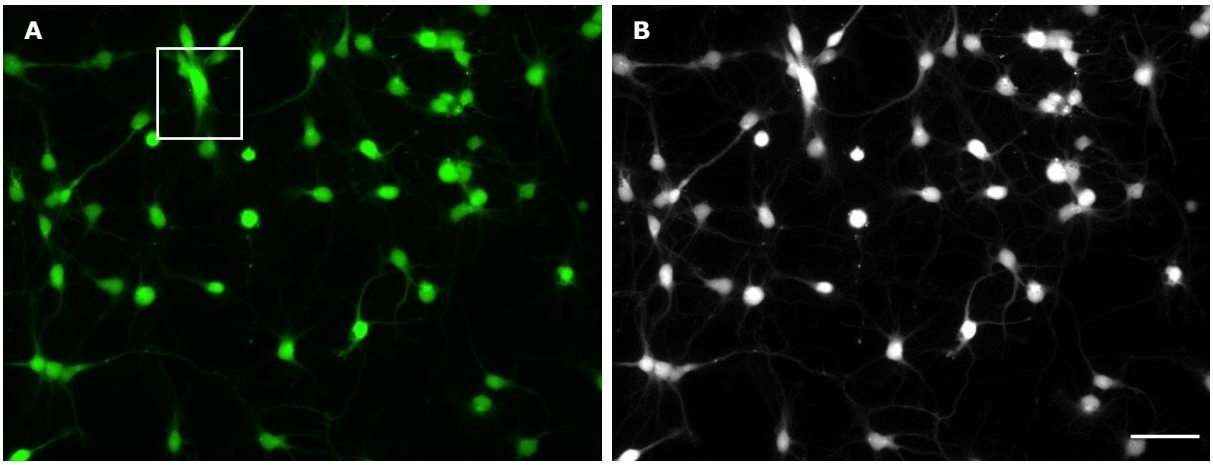

Figure 10 Cell loading with Fluo-4 AM calcium dye in P5 cells at DIV7. (A) Green channel. (B) Grayscale image. Inset shows protoplasmic astrocyte. Scale bar, 50 µm.

Calcium dye is very sensitive to light exposure, so prolonged imaging results in increase of the noise due to the dye bleaching. Cells with higher initial dye intake downgraded their intensity with prolonged light exposure. To attenuate the cell saturation and bleaching, and to protect the cells from phototoxicity, neutral density filters 25ND25 and 50ND50 were used. The correct balance between the use of the appropriate ND filter and setting of the CCD camera exposure time is fundamental because, if not appropriately chosen, calcium bursts may not be visualized. For instance, with 50ND50 ND filter and 100 ms exposure, calcium bursts are not recorded, and background noise may be seen. Therefore, compromise in attenuation of the light intensity has been made, by decreasing ND filter strength to 25ND25. 100 ms exposure was chosen as the best option because it can record calcium bursts and waves with sufficient time resolution. Time delay between each frame is the set exposition added with 0.017 s, which is the time necessary for one image to be acquired.

4.3. Functional maturation of primary cell cultures performed with calcium imaging

Functional maturation of cells and cell networks was observed mostly in P5 primary cultures, at several time points. P18 primary cell cultures were examined at DIV7 and compared to P5 cultures to test the change in maturation using opossums of different developmental stage.

In P3-5 cortical opossum cultures at DIV7, frame with high cell density was chosen (Figure 11C). Five of the cells were selected (Figure 11C, circled cells) showing the spontaneous activity, as observed by time-lapse recordings. Both frequency and pattern of activity were variable, but rhythmic synchronicity between cells may be detected (Figure 11B). Fluorescence intensity increased 2.5-fold compared to minimum of detectable cell activity. Cell activity is minimal for chosen cells at the beginning of exposure and greatest around second minute of recording. Synchronicity in calcium flux may be seen in neighboring cells (Figure 11B, orange, green and blue curves). Calcium activity shows different pattern for other cells, although to some point, synchronicity is preserved (Figure 11C, red and purple curves).

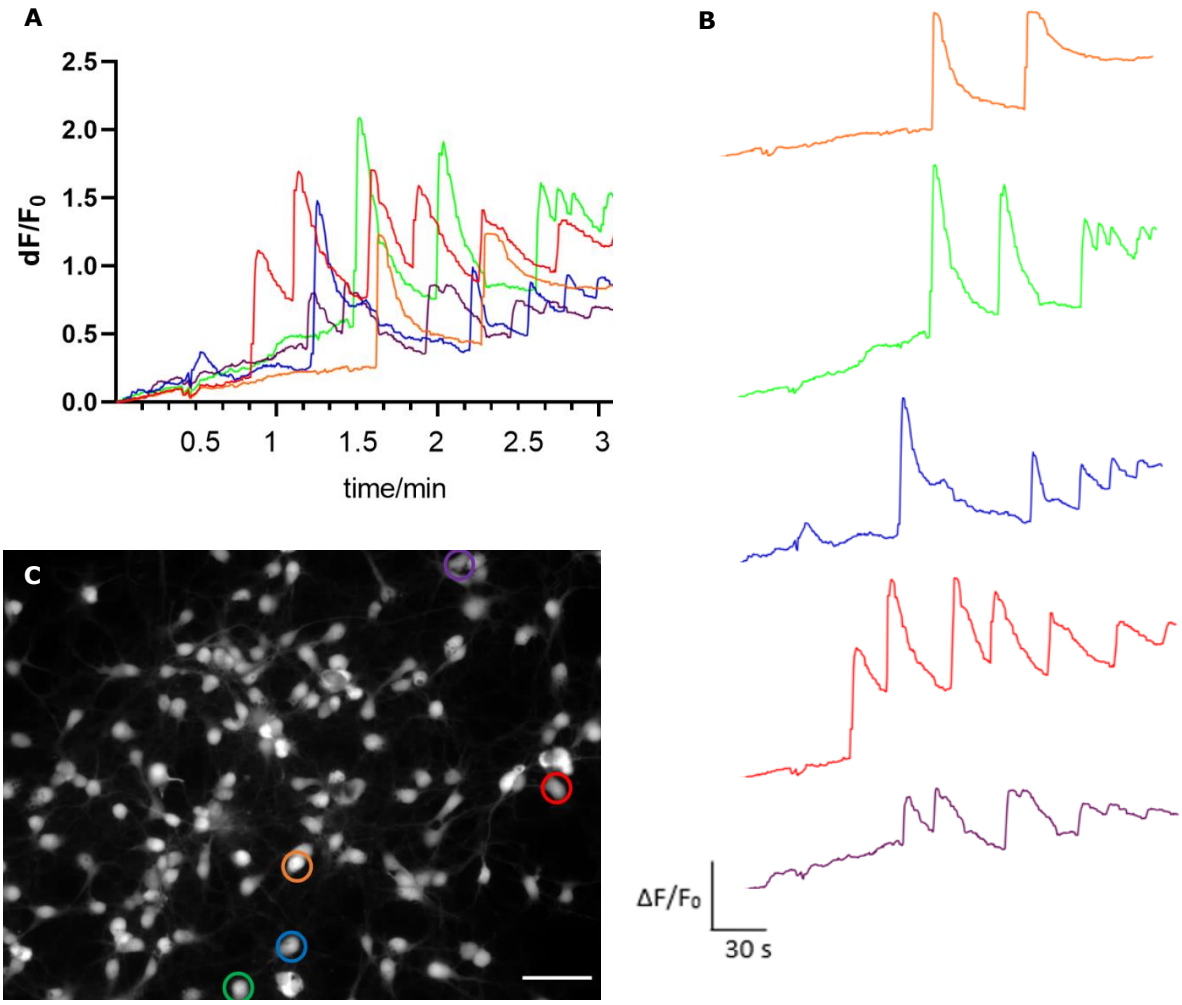

Figure 11 Spontaneous calcium activity in P3-5 cortical-derived primary cultures of M. domestica. (A) Recordings of spontaneous calcium fluctuations in five chosen cells presented as a relation of change in fluorescence intensity with time. (B) Graphical presentation of change in fluorescence intensity with time of isolated cells. (C) Location of selected cells in the sample. Scale bar, 50 µm.

To further investigate network connectivity, two more nearby cells with significant activity were chosen (Figure 12A). Initially, cell activity is not synchronized (Figure 12B). However, from approximately one minute after the beginning of the experiment, synchronized cell activity may be seen. Calcium firing of one neuron may provoke firing of second neuron, followed by synchronized activity in both neurons.

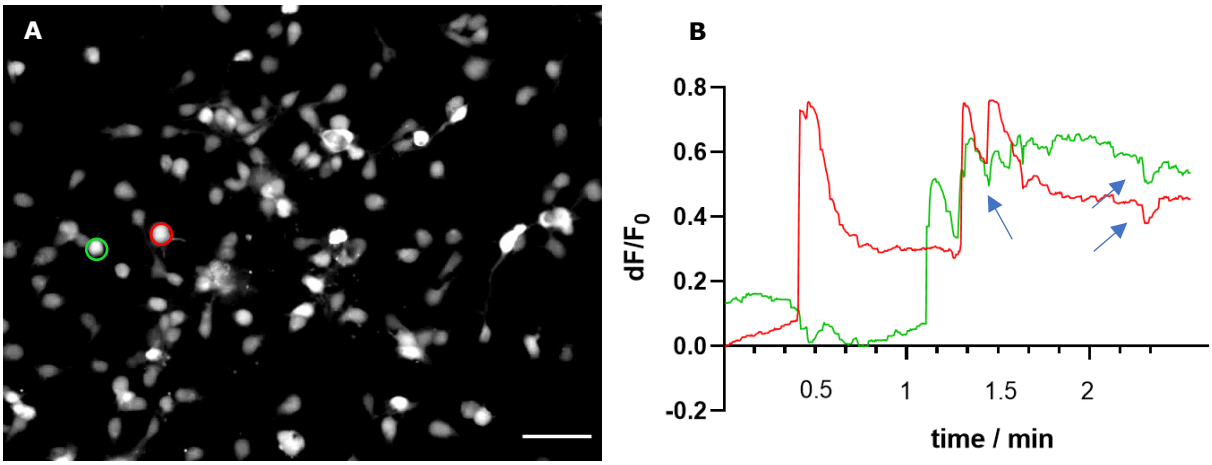

Figure 12 Spontaneous calcium activity of nearby cells in P3-5 cortical-derived primary cultures of M. domestica *at DIV7. (A) Location of selected cells in the sample. Scale bar, 50 µm. (B) Recordings of spontaneous calcium fluctuations in five chosen cells presented as a relation of change in fluorescence intensity with time. Arrows are pointing to synchronized calcium activity of neighboring cells.*

In P16-18 opossum culture, frame with the similar cell density as in P3-5 sample was chosen. Calcium flux may be seen in both soma and neurites of neurons as well as in astrocytes. Interestingly, in some cases, calcium propagation is observed in axons, while soma showed low activity. Five random cells were chosen (Figure 13C) and time-lapse recordings showed spontaneous oscillations in all selected cells (Figure 13A). Calcium activity frequency and pattern vary among cells. Selected cells had lower synchronous activity, correlating to greater distances. Fluorescence intensity increased between 0.5-1.5-fold respect to baseline. At the beginning of recording, four of the chosen cells showed minimal calcium activity. In contrast, one cell showed higher initial activity, followed with activity decline as experiment progressed (Figure 13B, orange curve). Neighboring cells showed low activity (Figure 13 A, B, green and blue curves). Synchronized activity with neighboring cells is visible only at one time point (Figure 13B, arrows), but is not that significant. One of the neighboring cells had 1.0-fold fluorescence intensity increase correlated with the increase in calcium activity in other two distant cells. This might suggest that the distant cells evoked the activity of one of the neighboring cells.

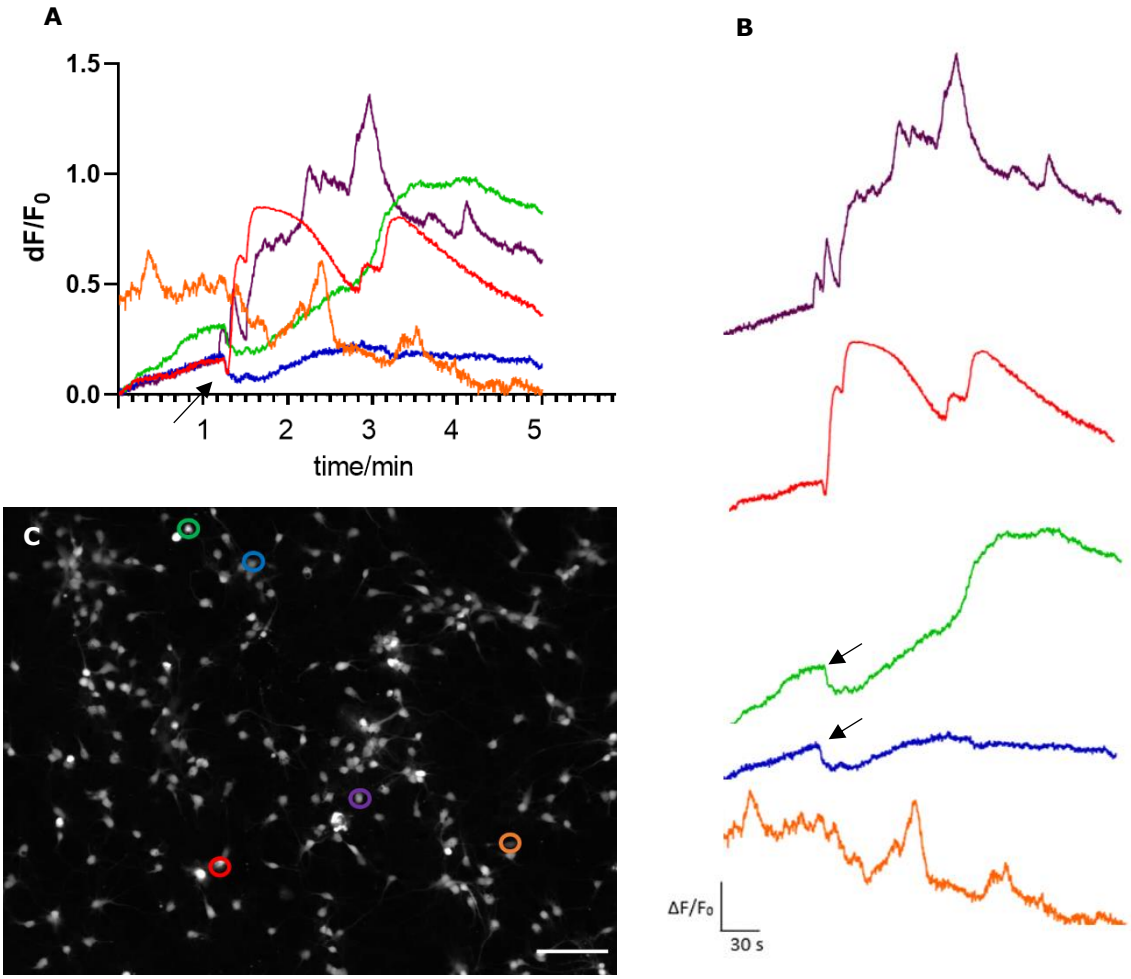

Figure 13 Spontaneous calcium activity in P16-18 cortical-derived primary cultures of M. domestica *at DIV7. (A) Recordings of spontaneous calcium fluctuations in five chosen cells presented as a relation of change in fluorescence intensity with time. Arrow is pointing to an activity pattern in cells. (B) Graphical presentation of change in fluorescence intensity with time of isolated cells. Arrows are pointing to an activity pattern in cells. (C) Location of selected cells in the sample. Scale bar, 100 µm.*

4.4. *In vitro* regeneration of primary cell cultures after an injury using immunocytochemistry

One of the ultimate goals of this work is to develop *in vitro* injury that could allow the study of (neuro)regeneration capacity of opossum primary cortical cultures. This was performed by scratch assay in both P3-5 and P16-18 primary cultures, as described in Methods. 24 hours after an injury is performed at DIV7 (Figure 14), first axonal extensions through the cut are visible (Figure 14, arrows). Some neurons extend their axons in parallel to the injury. In P3-5 cultures, clusters of $SOX9^{+}$ astrocytes are noted (Figure 14 A, inset), suggesting their induced proliferation following injury. In both P3-5 and P16-18 samples, cell nuclei are found in the middle of the injuries. They do not express neither neuronal nor astrocyte markers, and considering their small nuclear size, they ought to be dying cells.

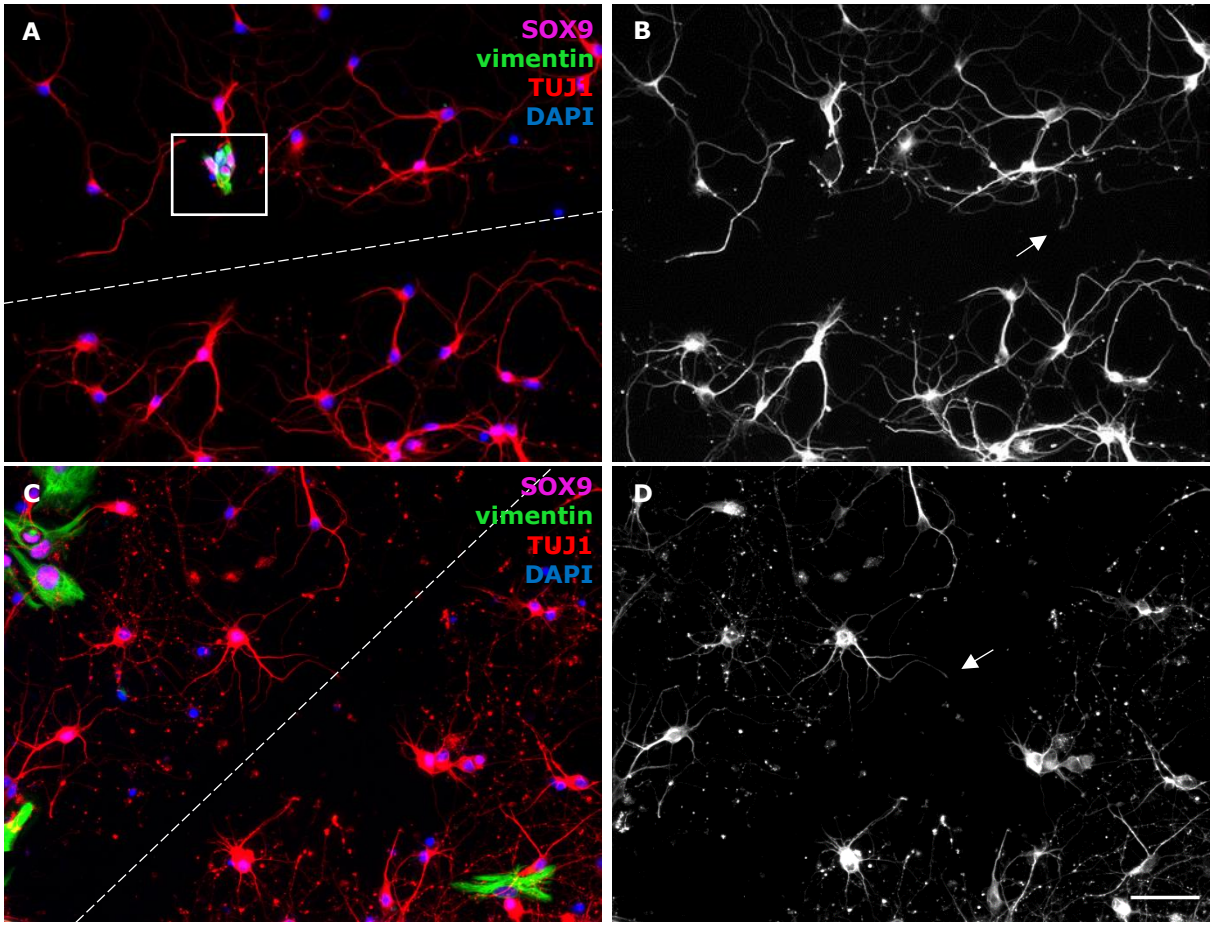

Figure 14 Primary cortical cultures fixed 24 hours after the injury at DIV7 from (A, B) P3-5; (C, D) P16-18 opossums. Cultures are stained for βIII-tubulin (TUJ1, red), vimentin (green), SOX9 (magenta) and nuclear stain DAPI (blue). (A) Inset is indicating the astrocyte cluster. (B, D) Grayscale images of βIII-tubulin for better visualization. Arrows are indicating to axons which are extending through the cut area. (A, C) Dashed line represents the injury location. Scale bar, 50 μm.

48 hours after injury, performed at DIV7 of P3-5 primary cultures (Figure 15), connections between both sides of the injury are formed (Figure 15B, F, arrows). Neurons nearby the injury extend to great distances parallel to the injury. $SOX2^{+}vim^{+}$ protoplasmic astrocyte is located next to the injury extending its processes parallel to the injury (Figure 15C). Interestingly, both $SOX9^{+}$ and $SOX9^{-}$ protoplasmic astrocytes

have migrated to the middle of the injury. Neuronal axons from both sides of the injury are extending over the astrocytes and follow their morphology.

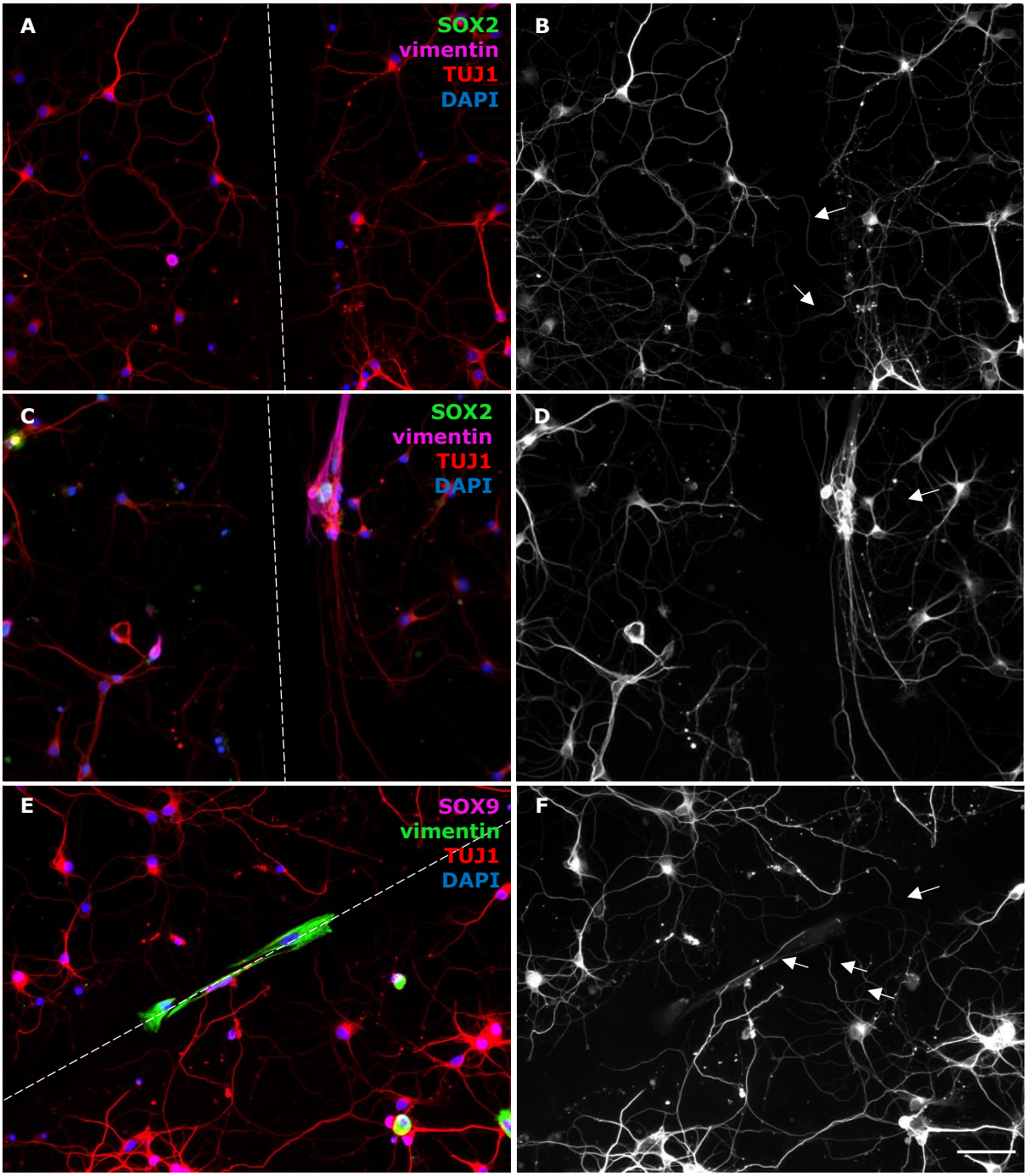

Figure 15 Primary cortical cultures from P3-5 opossums fixed 48 hours after the performed injury at DIV7. Cultures are stained for (A) βIII-tubulin (TUJ1, red), vimentin (magenta), SOX2 (green) with nuclear stain DAPI (blue); (B) βIII-tubulin (TUJ1, red), vimentin (green), SOX9 (magenta) with nuclear stain DAPI (blue). (B, D, F) Grayscale images of βIII-tubulin for better visualization. Arrows are indicating to axons which are extending through the cut area. (A, C, E) Dashed line represents the injury location. Scale bar, 50 µm.

In P16-18 cultures, 48 hours after the injury (made at DIV7, Figure 16), axonal connections between both sides of the injury have formed as well (Figure 16 B, D, F, arrows). Across the sample, axonal extensions are more prominent in comparison to P3-5 cultures at the same time point. Both protoplasmic and stellate astrocytes surround the injury area. Stellate astrocytes extend their long processes parallel to the injury (Figure 16 A, E), but also cross the injury site perpendicularly (Figure 16 E). Axons follow the astrocyte vim^{+} filament's orientation and extend parallelly to the injury across the sample, as in younger cultures.

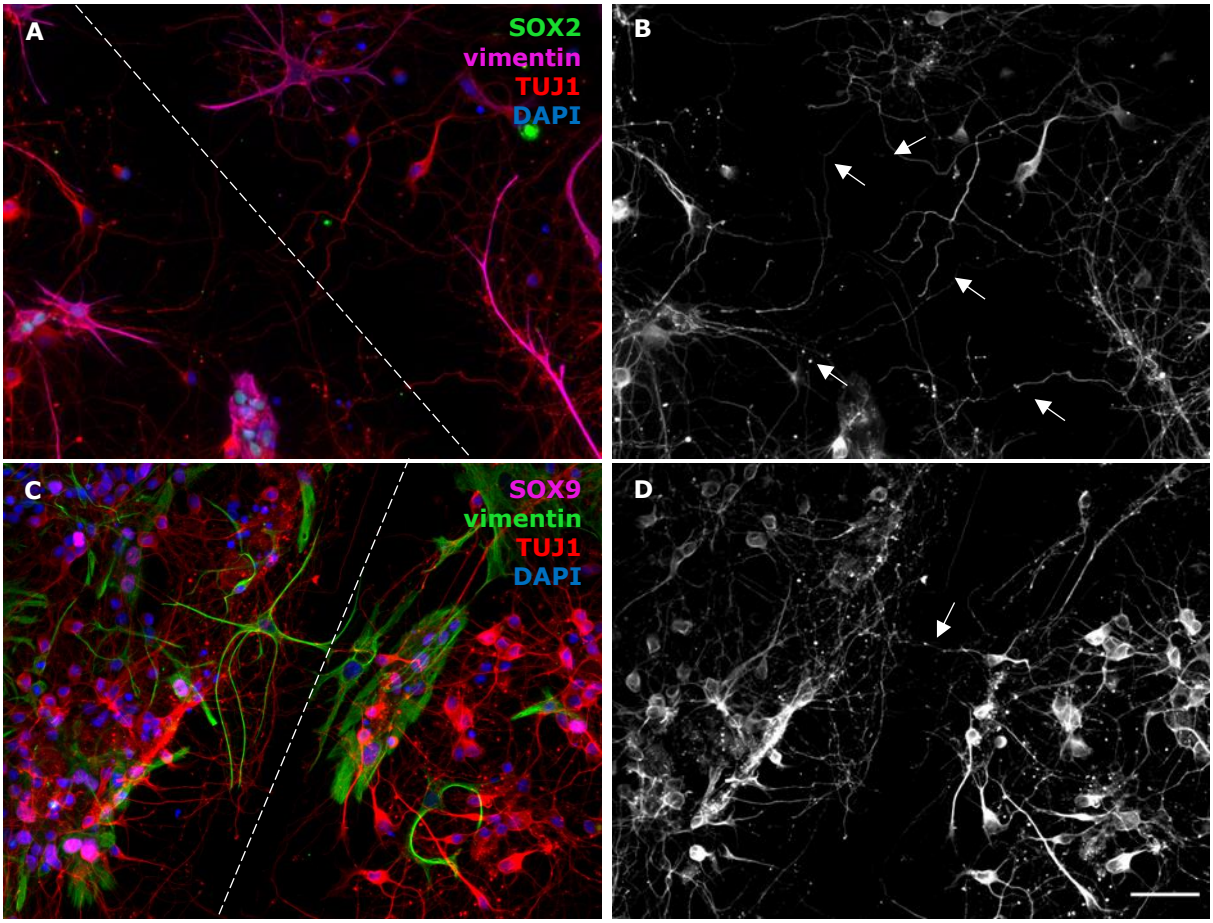

Figure 16 Primary cortical cultures from P16-18 opossums fixed 48 hours after the performed injury at DIV7. Cultures are stained for (A) βIII-tubulin (TUJ1, red), vimentin (magenta), SOX2 (green) with nuclear stain DAPI (blue); (C) βIII-tubulin (TUJ1, red), vimentin (green), SOX9 (magenta) with nuclear stain DAPI (blue). (B, D, F) Grayscale images of βIII-tubulin for better visualization. Arrows are indicating to axons which are extending through the cut area. (A, C) Dashed line represents the injury location. Scale bar, 50 μm.

When injury was performed at DIV10 in both P3-5 and P16-18 cultures, 24 hours after injury, axonal extension through the injury area is again observed. Axons extend parallel to the injury as well (Figure 17A). This extension is visible in most of the sample and results in reduced size of the injury. In both cultures, astrocytes migrate to the middle of the injury and surround the injury site. In P16-18 cultures, astrocytes form a glial-scar-like clusters. Astrocytes nearest to the cut orient parallelly to the cut, while more distant astrocytes spread their processes (Figure 17 C). Interestingly, those astrocytes were not SOX2^{+}.

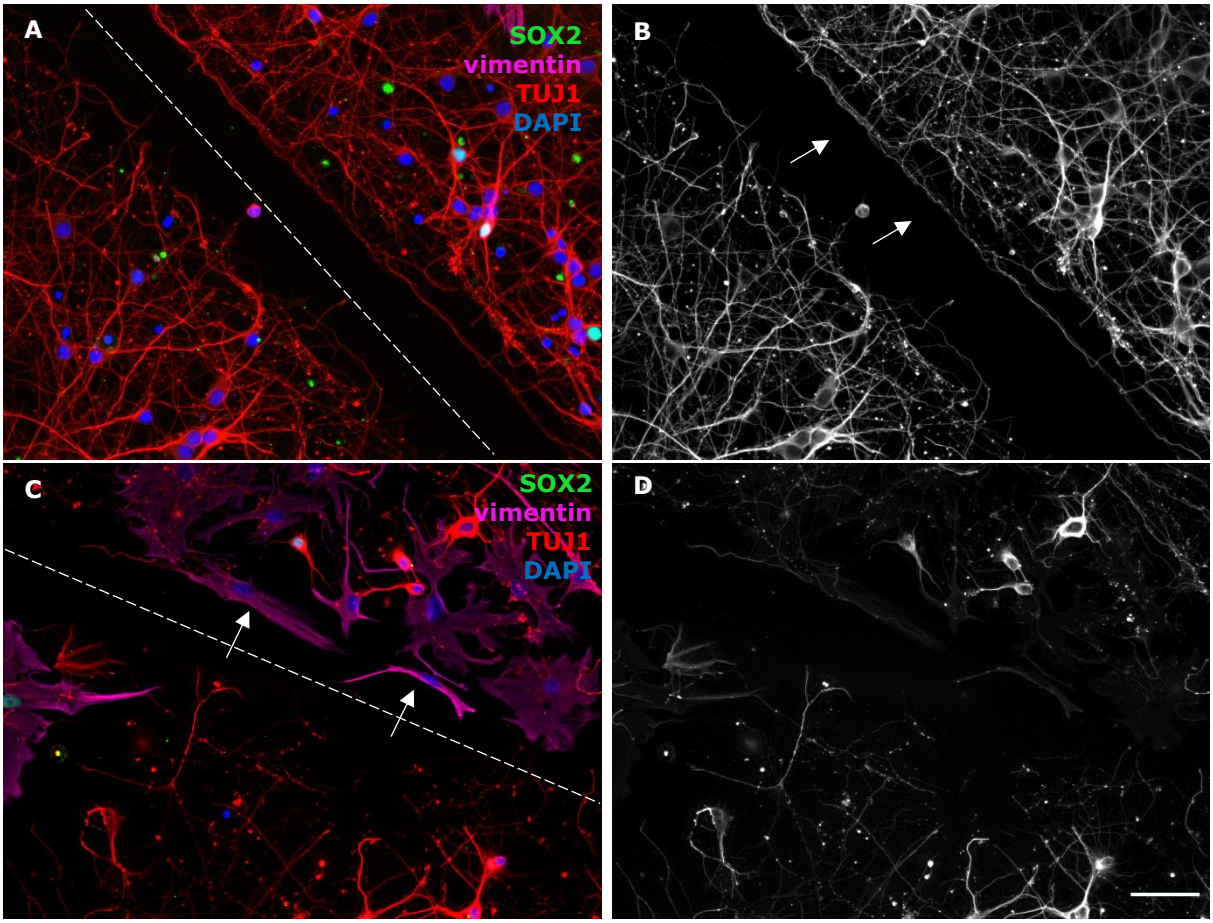

Figure 17 Primary cortical cultures fixed 24 hours after the performed injury at DIV10. Cultures are stained for βIII-tubulin (TUJ1, red), vimentin (magenta), SOX2 (green) with nuclear stain DAPI (blue). (A) P3-5 cultures. Dashed line represents the injury location. Arrows indicating to axonal extension parallel to the injury. (C) P16-18 cultures. Arrow indicating to glial-scar-like formation. (B, D) Grayscale images of βIII-tubulin for better visualization. (A, C) Dashed line represents the injury location. Scale bar, 50 μm.

Astrocyte proliferation is clearly visible 48 hours after injury of P3-5 cultures, performed at DIV10 (Figure 18). Most of them express SOX2. Stellate astrocytes have migrated to the middle of the injury and connect the two sides. Neurons have migrated to the middle of the cut and are placed parallelly to the astrocytes and the cut or vertically, extending their axons to connect the opposite sides. As a result, the size of the injury is visibly reduced.

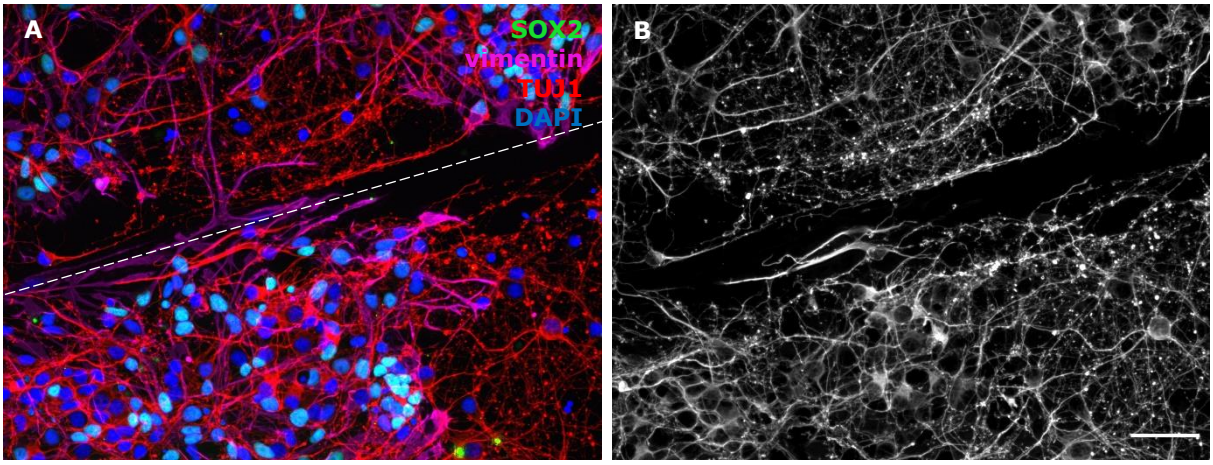

Figure 18 Primary cortical cultures from P3-5 opossum fixed 48 hours after the performed injury at DIV10. Cultures are stained for βIII-tubulin (TUJ1, red), vimentin (magenta), SOX2 (green) with nuclear stain DAPI (blue). Dashed line represents the injury location. (B) Grayscale image of βIII-tubulin for better visualization. Scale bar, 50 μm.

P16-18 cultures, injured and fixed at the same time point as P3-5 cultures show significant astrocyte proliferation and glial-scar-like formation surrounding the cut area (Figure 19 A, C). Interestingly, as in P16-18 cultures cut at DIV10 and fixed 24 hours later, astrocytes that form the glial-scar-like formation do not express SOX2. Moreover, throughout the sample, clusters of astrocytes near the cut express SOX2. Both astrocytes that express and do not express SOX9 surround the cut area. $SOX9^+$ astrocytes are not as clustered as $SOX2^+$ astrocytes (Figure 19 A, C).

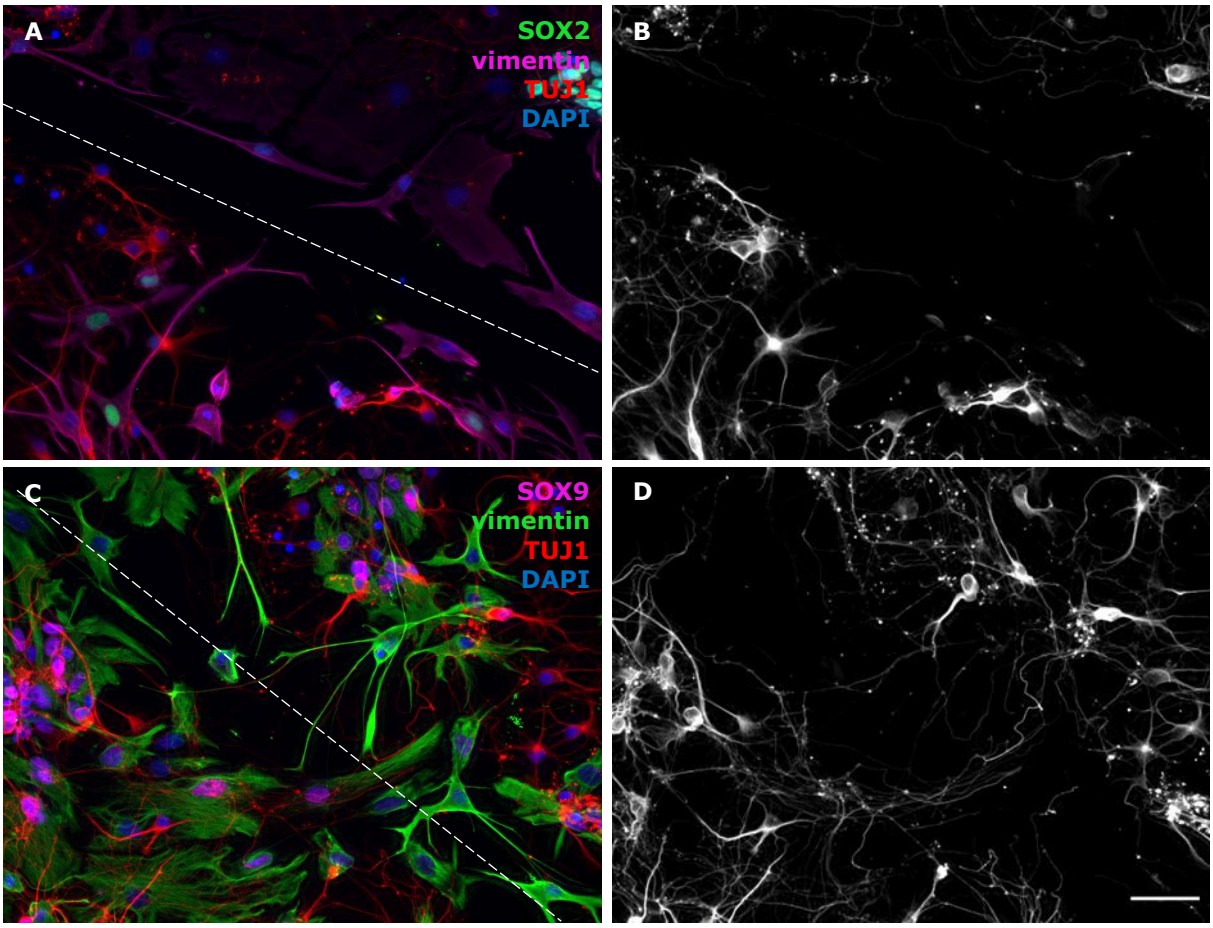

Figure 19 Primary cortical cultures from P16-18 opossums fixed 48 hours after the performed injury at DIV10. Cultures are stained for (A) βIII-tubulin (TUJ1, red), vimentin (magenta), SOX2 (green) with nuclear stain DAPI (blue); (C) βIII-tubulin (TUJ1, red), vimentin (green), SOX9 (magenta) with nuclear stain DAPI (blue). (B, D) Grayscale images of βIII-tubulin for better visualization. (A, C) Dashed line represents the injury location. Scale bar, 50 µm.

To check the regeneration capacity over time, an injury was performed at DIV14 of P3-5 cultures. After 24 hours, cultures resembled the ones where injury was performed at DIV10 and analyzed 48 hours after injury. The injury size reduced again, due to the axon extension and astrocytes that migrated into the cut area. 48 hours after an injury performed at DIV14, the injury size was significantly reduced (Figure 20 C, D). The cells formed numerous connections between the opposite sides of the injury (Figure 20 A, B). Interestingly, more connections are made in locations with fewer astrocytes surrounding the injury, but were also evident in locations with astrocytes.

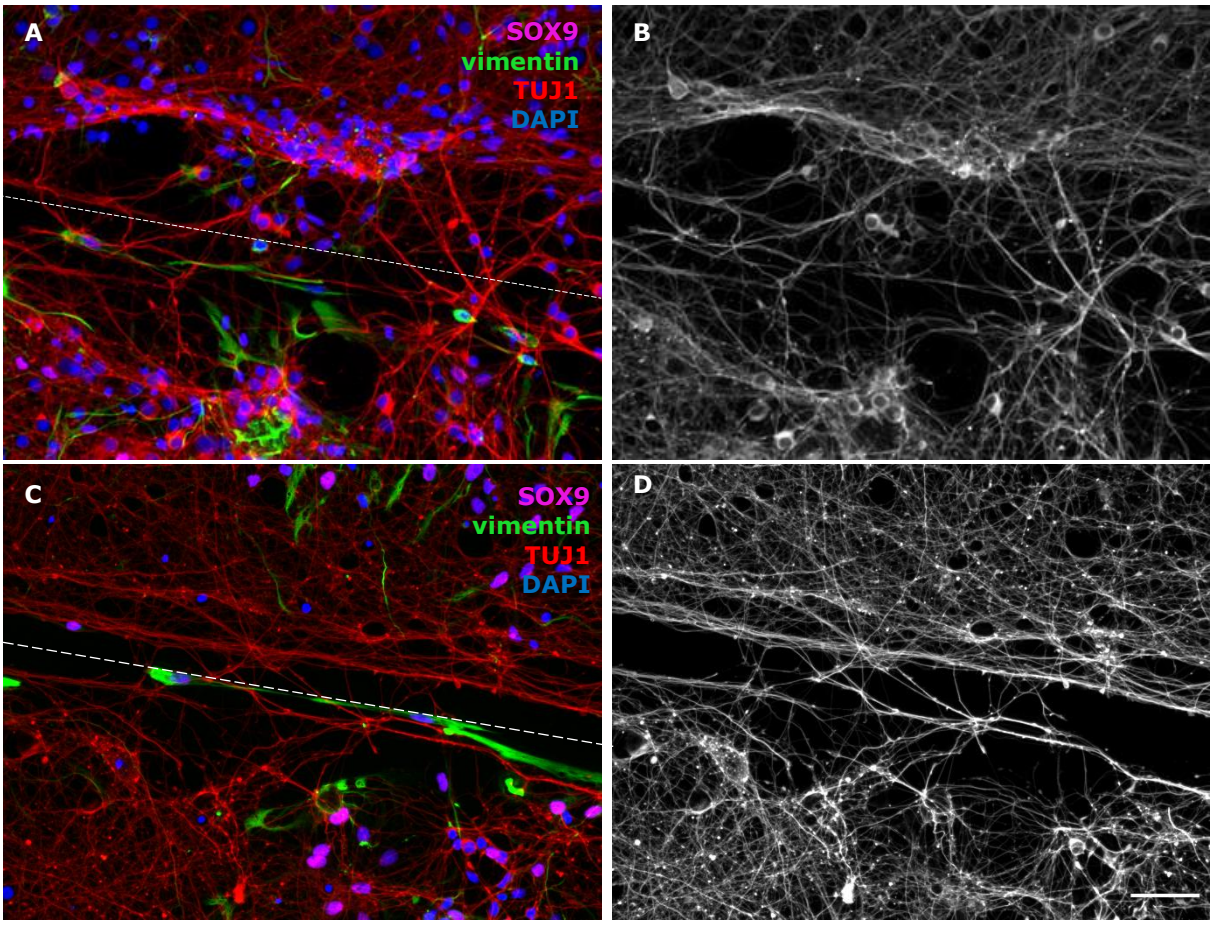

Figure 20 Primary cortical cultures from P3-5 opossums fixed 24 hours after the performed injury at DIV14. (A, C) Cultures are stained for βIII-tubulin (TUJ1, red), vimentin (green), SOX9 (magenta) with nuclear stain DAPI (blue). Dashed line represents the injury location. (B, D) Grayscale images of βIII-tubulin for better visualization. Scale bar, 50 μm.

Less neurons are viable in DIV14 of P16-18 cultures and injury may have triggered increased cell death, therefore these cultures have reduced number of cells and axonal extensions throughout the sample. 24 hours after an injury, glial-scar-like formation is observed (Figure 21 A). Notably, glial-scar-like formation in these cultures was forming in the reduced width of the injury (Figure 21 A, arrows). In these cultures, astrocytes forming the glial-scar-like formation and surrounding neurons were $SOX2^{+}$ (Figure 21A).

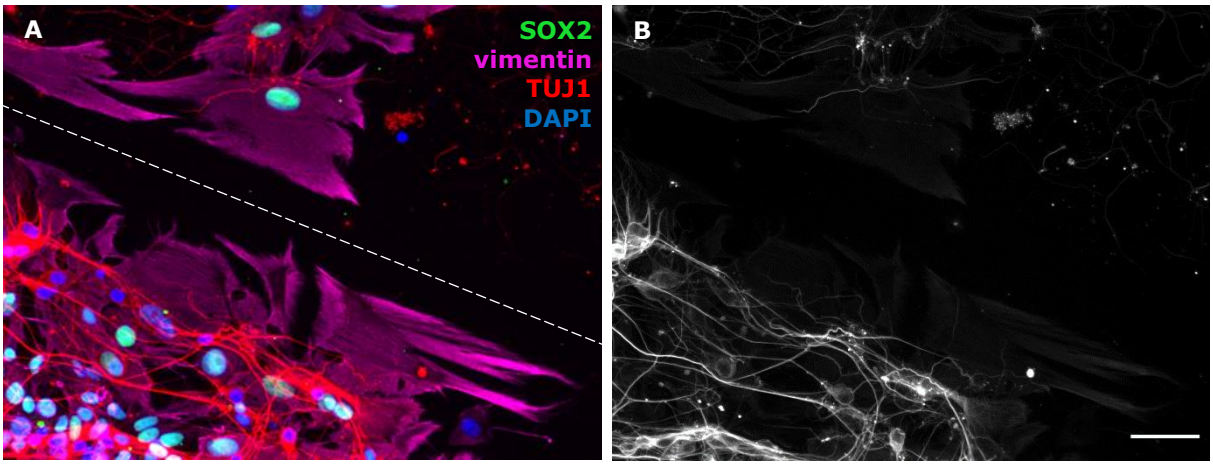

Figure 21 Primary cortical cultures from P16-18 opossums fixed 24 hours after the performed injury at DIV14. Cultures are stained for (A) βIII-tubulin (TUJ1, red), vimentin (magenta), SOX2 (green) with nuclear stain DAPI (blue). Dashed line represents the injury location. (B) Grayscale image of βIII-tubulin for better visualization. Scale bar, 50 μm.

4.5. *In vitro* regeneration of primary cell cultures after an injury using calcium imaging

In P3-5 cultures, an injury was performed at DIV10. Calcium imaging was obtained 48h and 72h after an injury. Random frames surrounding the location of injury were selected for imaging.

48h after injury, calcium activity was detected in almost every cell in the frame in cell soma and axons. Calcium propagation through axons was observed. Five random cells were selected from both sides of the injury (Figure 22C). Time-lapse of calcium activity showed strikingly synchronized calcium activity in all cells (Figure 22A). Both calcium flux frequency and pattern are the same in all cells in the first and a half minute of recording. Following that, pattern of activity remains the same, but some variations in activity are observed among the cells. Around 0.4-fold of increase in fluorescence intensity is observed and the activity was detected already at the beginning of the recording. Interestingly, after 0.5 min, the sudden drop of activity in all cells was observed. In the following minute, transient rise of calcium activity was detected. After that, a decline in calcium activity was observed.

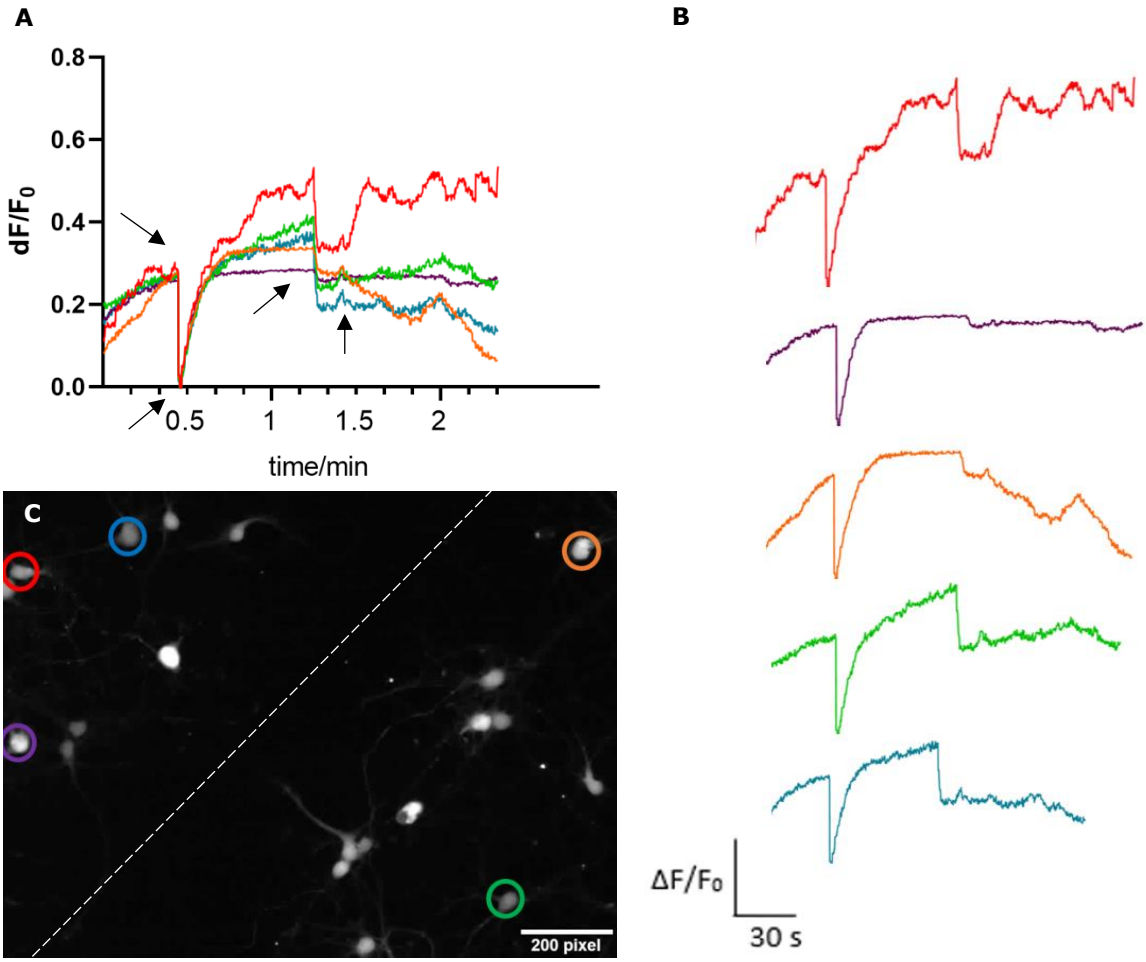

Figure 22 Calcium activity in P3-5 cortical-derived primary cultures of M. domestica *48h after the performed injury at DIV10. (A) Recordings of spontaneous calcium fluctuations in five chosen cells surrounding the injury site presented as a relation of change in fluorescence intensity with time. Arrows are pointing to an activity pattern in cells. (B) Graphical presentation of change in fluorescence intensity with time of isolated cells. (C) Location of selected cells in the sample. Dashed line presents the injury location. Scale bar, 50 µm.*

When the same calcium imaging experiment was performed 72h after injury, calcium flux was detectable in almost every cell in the selected frame, while some cells had axonal calcium propagation. Five cells were selected – two from each side of the injury and one located in the cut area (Figure 23). Calcium activity showed interesting results. Two different patterns of activity were detected. In the first minute, activity increased in two cells (Figure 23A, purple and red curve) and slightly decreased in the other three cells. At 1.5 min, all cells had rapid decrease in their activity, followed by a pattern of activity visible in all cells. Interestingly, the cell

located in the cut area had striking similarity in activity pattern with cells located on the other side of injury (Figure 23C, blue curve). This may indicate that cell develop certain degree of rhythmic activity that persist after injury, despite the fact that those cells have lost their original connections. An increase of fluorescence intensity was around 0.4-fold for all cells and detected activity was more significant in the first four minutes of experiment, after which stagnation in calcium flux was observed.

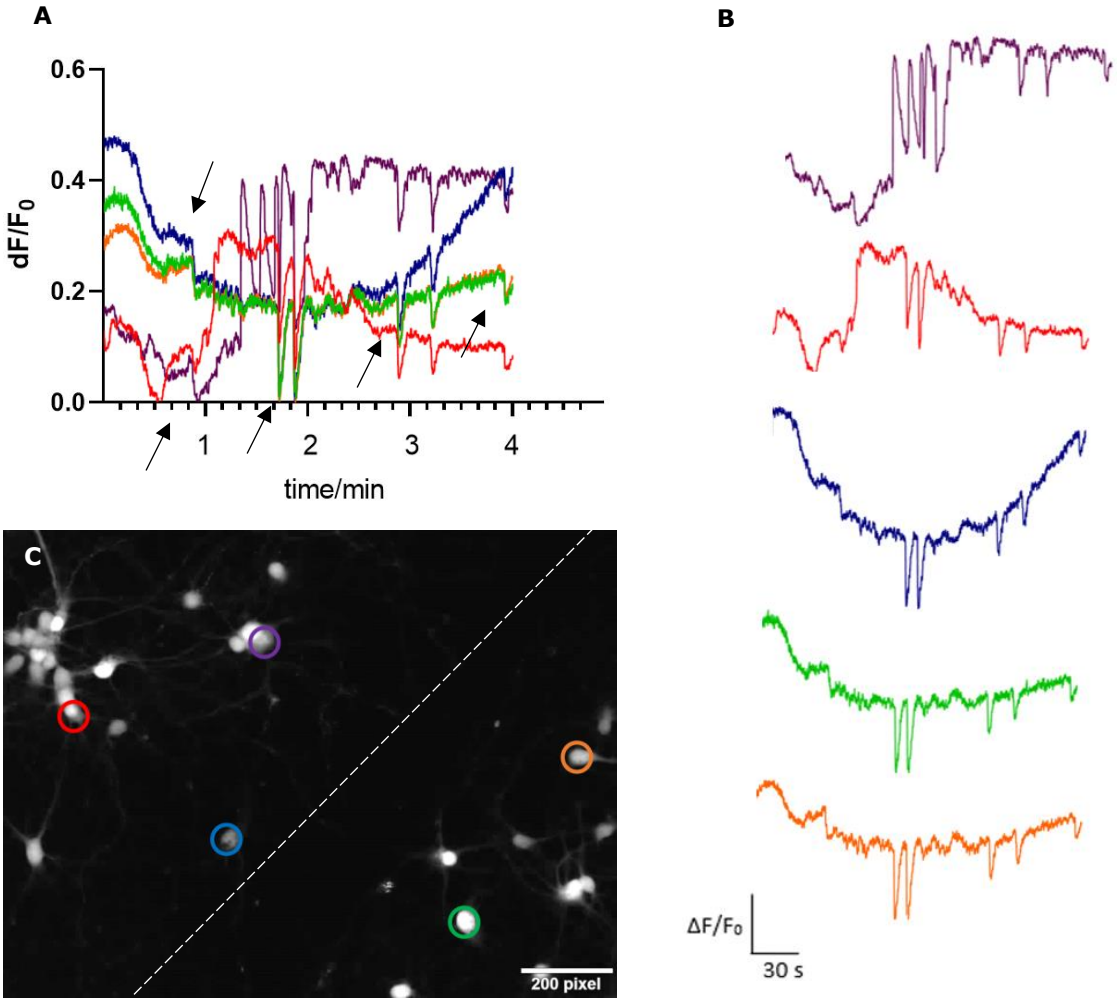

Figure 23 Calcium activity in P3-5 cortical-derived primary cultures of M. domestica *72h after the performed injury at DIV10. (A) Recordings of spontaneous calcium fluctuations in five chosen cells surrounding the injury site presented as a relation of change in fluorescence intensity with time. Arrows are pointing to an activity pattern in cells. (B) Graphical presentation of change in fluorescence intensity with time of isolated cells. (C) Location of selected cells in the sample. White dashed line presents the injury location. Scale bar, 50 µm.*

5. Discussion

The complexity of mammalian CNS and its investigation requires additional models and methods of research. Continuous and/or immortalized cell lines derived from CNS precursors or tumor cells fail to fully reproduce axons, dendrites and synapses[45]. Primary neuronal cultures allow for neurons and glial cells to be maintained *in vitro* in less complex environment, but also available for *in vitro* manipulations. They have become essential for the research of complex and poorly understood mechanisms of CNS functioning at a molecular basis.

Primary neuronal cultures derived from *Monodelphis domestica* cortex can be successfully obtained from animals at different postnatal days. Different developmental ages of opossum have distinct cell environment and gene profile related to their ability to regenerate spinal cord after injury – otherwise not possible in the most of other postnatal mammals. Primary neuronal cultures allow us to investigate neuronal and glial differentiation and maturation, formation of synapses and cell networks *in vitro*. Moreover, opossum primary neuronal cultures may be manipulated with the choice of medium and supplements for cultivation, resulting in different CNS cell type composition. Therefore, we can consider opossum-derived cortical cultures as favorable model for mammalian CNS development and regeneration investigation.

In this thesis, opossum-derived cortical primary cultures were obtained from different age groups – P3-5 and P16-18. Age-dependent morphological and functional changes at different timepoints were explored. Moreover, an injury was performed at different time points *in vitro*, to study the cellular environment and response to an injury leading to the capability of opossum cortex regeneration.

Primary cortical dissociated cultures obtained from postnatal opossums attached and survived well allowing extended, i.e. long-term culturing period. P3-5 cultures were viable in culture for more than a month,

while P16-18 cultures were viable between three and four weeks upon cultivation. Older cultures had more dead cells and debris and are more susceptible to damage, considering they have more mature CNS cells than younger opossum cultures. Older cultures also have more adherent meninges leading to the increased presence of fibroblasts and cell debris[45]. To overcome this issue, preplating step is introduced to primary cell cultivation, significantly reducing the cell debris.

The cell survival, growth and maturation was observed in both age groups of opossum-derived cortical cultures. One day upon plating, neurons formed neurites and growth cones at their endings. Neurons continued growing their processes and became arborized after a few days in culture. In DIV7, neuronal connections with nearby neurons and astrocytes are visible. Expression of synaptic markers was confirmed as well[44]. Cell morphology became more complex for both neurons and astrocytes. Neurons were arborized with a long axons and multiple dendrites. Astrocytes had more elaborate processes and could be divided morphologically into protoplasmic and stellate astrocytes. The percentage of neurons slightly diminished due to proliferation of glial cells in culture.

Several markers involved in maturation and development were used. Neuronal cytoskeletal marker of choice was TUJ1 that stains a specific tubulin isoform expressed in immature neurons[35]. It is very specific to opossum-derived neurons and shows neuronal cytoskeleton from perinuclear area to the axon and fine dendrites. Coupled with phalloidin stain for F-actin, morphological changes in developing neurons can be observed, such as formation of growth cones and formation of dendritic spines (Figure 5). *In vitro* maturation of cells as well as transition from progenitor cells to differentiated cell phenotype was studied using SOX2, SOX9, vimentin and GFAP markers.

CNS progenitor cells were monitored with SOX2 marker. SOX2 is expressed during the embryonic CNS development and in progenitors in germinative areas throughout the life[46]. Ellis et al.[48] have shown that SOX2

acts as a neural stem cell marker and that SOX2-expressing cells are multipotent self-renewing cells. Interestingly, SOX2 is expressed in almost 50% of the cells in P3-5 cultures and in around 30% of the cells in P16-18 cultures at DIV7. $SOX2^+$ cells decrease with cultivation *in vitro* and with increase in glial cell number. Interestingly, $SOX2^+$ cells were observed in co-expression with TUJ1, in contrast to previous evidences that report that $SOX2^+$ cells are exclusive of TUJ1[30]. We have obtained around 30% of $SOX2^+TUJ1^+$ cells in P3-5 cultures and around 3% of cells in P16-18 opossum cultures at DIV7. Additional research has identified $SOX2^+TUJ1^+$ cells as neuronal-progenitor cells localized in SVZ[30]. Therefore, our findings suggest that SOX2 expression in opossums persist in post-mitotic neurons, and we cannot exclude the additional role of SOX2 in early neuronal differentiation as well. Since cell composition with highest amount of $SOX2^+$ and $SOX2^+TUJ1^+$ cells is obtained at DIV11 of P3-5 cultures, this is in good agreement with peak of neurogenesis that for opossums is considered to occur around P16[40]. In addition, this finding supports the development timeline being similar in *in vitro* conditions to development *in vivo.*

$SOX2^+TUJ1^-$ cells are present in 15% of the cells of P3-5 cultures and in 27% of cells in P16-18 cultures at DIV7. These cells ought to be progenitors that can differentiate into neurons, but also in glial cells[46]. $SOX2^+TUJ1^-$ cell expression declines with cultivation and differentiation of progenitors into neurons and glial cells, as expected.

SOX9 expression emerges in NPCs before gliogenesis initiation in embryonic development of CNS and stays expressed in NPCs in the adult CNS[36]. SOX9 is expressed in 16% of cells in P3-5 cultures and in 22% of cells in P16-18 cultures at DIV7. The highest number of $SOX9^+$ cells is present in DIV16 of P3-5 cells. This results support the finding that gliogenesis begins in P18 opossums[40], as well as the similar timeline of maturation *in vitro* to *in vivo* conditions. SOX9 expression is highest in DIV7 of P16-18 cultures. It decreases with cultivation considering the reducing number of NPCs in more mature cultures[36]. Almost every cell in both age

groups are SOX9$^+$vim$^+$, supporting the differentiation of NPCs into glial cells. Less than 2% of cells in both cultures are SOX9$^+$vim$^-$. These cells could represent more mature state of astrocytes that have downregulated vimentin and that retain SOX9 expression, as observed in the adult brain[49].

Astrocyte maturation is observed by comparing GFAP and vimentin expression at DIV7 of P3-5 and P16-18 cultures. Both cultures had stellate and protoplasmic astrocytes, but protoplasmic astrocytes were more common. Astrocytes in P3-5 cultures were thinner and showed less elaborated processes, while in P16-18 cultures, astrocytes were more complex with elaborated processes. Higher number of vim$^+$ cells was observed in both cultures. Younger cultures in every GFAP$^+$ cell co-expressed vimentin, while in older cultures, GFAP$^+$vim$^-$ astrocytes have emerged, proving the *in vitro* maturation of astrocytes with downregulation of vimentin[34].

To study the functional connectivity of cells and the formation of functional neuronal networks, calcium imaging was performed. To best of our knowledge, calcium imaging has never before been conducted on opossum-derived primary neuronal cultures, so this work presents first insight into functional analysis of primary neuronal cultures and regeneration after an injury for *M. domestica*.

Calcium imaging protocol had to be established and optimized. Imaging of samples was performed in an incubator chamber with temperature set at 32.5°C. Chosen calcium indicator was Fluo-4 AM, which is a single-wavelength calcium indicator, displaying fluorescence change when a change in emission of Ca^{2+} signals occurs[50]. A setback of single-wavelength indicators is that they are not adequate for analysis of individual cell amounts of intracellular calcium, as the neighboring cells usually do not have the same initial uptake of the indicator[50]. However, single-wavelength indicators provide the platform for measuring relative changes in calcium ion concentration in cells. Fluorescence signal is expressed as a relation to its baseline signal, dF/F_0. Baseline signal can be measured as a signal at

the initial point of experiment, or minimum of fluorescence. For the purpose of this preliminary research, F_0 is calculated as the average of six neighboring intensities of the minimum of fluorescence for each cell.

Considering these were first attempts in the calcium imaging of primary cortical cultures derived from *M. domestica*, as well as the first attempts in calcium imaging in general in our laboratory, wide-field imaging method was performed. Wide-field imaging had an advantage of simplicity, as well as more cells in a frame, but reduced information was gained as a result of reduced resolution, exposing more cells to light and out-of-focus signals acquired in some cells and frames.

Prolonged imaging results in increase of the noise due to the dye bleaching of cells and background. Photobleaching occurs because indicator in excited state reacts with oxygen, producing a non-fluorescent molecules[50]. Cells often raise their fluorescence signal with prolonged light exposure, but some cells with higher initial dye intake downgraded their intensity with time. To attenuate the cell saturation and bleaching, and to protect the cells from phototoxicity, neutral density filters were used. The correct balance between the use of the appropriate ND filter and setting of the CCD camera exposure time is fundamental because if not appropriately chosen, calcium bursts may not be visualized.

Calcium activity sampling rate was set at 3–10 Hz with a spatial resolution of 1344 x 1024 pixels obtaining 8-bit movies in .avi format. With this setup of calcium imaging method, visualization of neuronal and astrocyte soma, neuronal axons and thicker neurites was possible. Calcium analysis was performed only for cell bodies, since with the wide-range imaging of axons and processes of single cells cannot be adequately visualized. Dying cells were also visualized with greater dye expression due to calcium ions being overloaded during the cell death[47]. With prolonged light exposure, cell death onset is visible to cells that previously were active and healthy-looking.

Cell network functionality and maturation were tested at DIV7 for P3-5 cultures and P16-18 cultures. In P3-5 cultures, spontaneous calcium activity was observed in cell soma and axons. Frequency and pattern of calcium activity varied among cells, but also synchronicity in calcium flux is detected. 2.5-fold increase to the detectable calcium cell activity was noted. Neighboring cells showed cell synchronicity in second part of experiment, but varied in the beginning of experiment. This could be a result of one neuron whose calcium firing may have provoked the calcium activity in the second neuron, following with further synchronized calcium activity in cells.

In P16-18 opossum culture, calcium activity was also visible in cell soma, axons, bigger dendrites and astrocytes. Spontaneous cell activity was detected in all five selected cells in the frame. Apart from P3-5 sample, this experiment was obtained with 10x objective, making chosen cells for spontaneous activity located at further distances. Time-lapse of spontaneous calcium activity showed more diversity in calcium transients, correlating to the bigger distances among cells. Cells also showed more activity than P3-5 cultures had at the same point of cultivation. Fluorescence intensity reached 0.5-to-1.5-fold increase of calcium cell activity. Interestingly, one cell had initial calcium activity bigger than other cells, followed by a decline in calcium activity. A result of this may be that this cell had bigger initial uptake of the indicator, which resulted in faster activity with oxygen producing non-fluorescent compounds, as discussed previously. Neighboring cells showed some synchronicity among, but the interesting part is that one of the neighboring cells seemed to have been provoked by other cells' activity, resulting in increased calcium activity.

Another functional assay performed to study the primary cortical cells and regeneration *in vitro* was the scratch assay. Cultures were transected in the middle of coverslip 24 and 48 hours after DIV7, DIV10 and DIV14 for P3-5 and P16-18 cultures. Transection was performed with 0.1 mm tip tweezers, making a cut of around 100 μm width.

At DIV7 samples of both age groups, 24 hours after the injury, first axonal extensions through the cut were observed. Some neurons extended their axons in parallel to the cut area, while some neurons extended their axons vertically to the cut. 48 hours after an injury, opposite sides of the cut are connected with extended axons. Astrocytes begin to migrate near the cut area and proliferate or migrate inside the cut area. Neuronal axons follow the astrocyte morphology in the cut area. Axonal extensions are more common in P16-18 samples.

At DIV10, 24 hours after an injury, axonal extension and astrocyte migration and accumulation around the cut are continued. Due to axonal orientation in parallel to the cut, the injury diameter reduces in both P3-5 and P16-18 cultures. In P16-18, glial-scar-like formation starts to be visible. Nearest astrocytes are placed parallelly to the injury, while further astrocytes spread their processes. Interestingly, these astrocytes did not express SOX2. It was reported that SOX2 is induced by TBI and that it regulates reactive astrocyte functions[51]. In addition, recent research have shown that conditional deletion of SOX2 in adult astrocytes significantly reduces injury area and lesion size, as well as improves functional recovery following the TBI[51]. 48 hours after an injury in P3-5, astrocytes proliferation is visible, as well as most cells expressing SOX2. Some neurons have fully migrated into the cut area and orientated vertically and parallelly to the injury. In P16-18 cultures, glial-scar-like formation around the injury does not express SOX2, but clusters or $SOX2^+$ astrocytes are visible near the injury across the sample. These astrocytes might be newly proliferated astrocytes which are regulated and induced with injury by SOX2[32].

After an injury performed in DIV14 samples, injury reduction and astrocyte accumulation were visible in P3-5 and P16-18 cultures. Numerous connections across the injury are visible in P3-5 cultures 48 hours after an injury. More connections are visible in places with reduced accumulation of astrocyte, supporting that glial scar acts as a physical and chemical barrier for CNS regeneration[2]. P16-18 cultures with injury performed at DIV14 had

reduced survival of cells because they are more susceptible to damage. However, in samples reduced diameter of injury and glial scar are observed, as well. Much less connections are made in comparison to P3-5 opossums, which might be a result of sooner formation of glial scar and reduced axonal extension across the injury. In these cultures, astrocytes that form glial scar and neurons near the injury express SOX2. This might be a result of cell reprogramming to progenitors due to increased cell death and injury[32].

Calcium imaging after an injury was observed in P3-5 cultures at DIV10. Experiments were obtained 48h and 72h after an injury. Experiments were conducted with the purpose of testing the cell network activity after an injury, so prolonged time-points after the injury were chosen, unlike in immunocytochemistry experiments. As mentioned in immunocytochemistry results, 24h after an injury, some neurons began to migrate and extend their axons in the cut area. 48h after an injury, axons begin to cross the entire cut area, extending to the other side forming connections.

48h after an injury was performed, calcium transients were present in almost every cell in the observed frame. Time-lapse of randomly selected cells surrounding the cut area showed a remarkable pattern of synchronicity among all cells. This indicated that 48h after an injury, cells managed to reconstitute their cell network. Calcium activity is the same for all cells in the first and a half minute, after which a slight variation in cell activity occurs. 0.4-fold of increase in fluorescence intensity is observed in cells. At 0.5 minute of filming, a sudden decline in cell activity was visible. This declines in calcium activity were visible in other experiments, at different days in culture and in cultures prepared from different postnatal ages, excluding the possibility of bugs in obtaining the video. More research should be conducted to study this phenomenon, but the probable explanations would be the calcium-dependent action potential and calcium-induced calcium release followed by decay[25].

72h after injury, sample showed calcium activity in soma of almost every cell and axonal calcium propagation in some cells. Time-lapse results of five selected cells showed two different patterns of calcium activity. Two of the cells at one side of the injury had the same activity pattern, while other two cells at different side of injury had the other calcium activity pattern. The cell that was in the cut area, approaching to the one side of the cut had the calcium activity pattern of cells from the other side of the injury. This cell had to migrate from one side to the other in the 72h period after an injury. Around 1.5-minute time point, a quick decrease in cell activity was observed, followed by a pattern of activity in all cells. Fluorescence intensity increase was around 0.4-fold for every selected cell. Detected activity was more prominent in the first four minutes of lamp exposure, following with calcium activity stagnation.

6. Conclusions

1. The long-term primary cortical neuronal cultures from neonatal opossum can be maintained up until a month after the tissue collection.
2. P3-5 opossum cortex gives rise to almost pure neuronal culture with more than 93% of neurons, while P16-18 cultures consist of 80% of neurons and 20% of glial cells.
3. At DIV7 cultures of both opossum age groups, neurons have formed synaptic connections and astrocytes become more evident.
4. Neural progenitor cells are prominent in opossum cultures of younger postnatal age and their number reduces with culture maturation. $SOX2^+$ cells represent 45% of P3-5 cultures and 30% of P16-18 cultures, at DIV7. $SOX2^+TUJ1^+$ cells are present in 30% of younger cultures, but in only 3% of older cultures.
5. $SOX9^+$ cells account for 16% of P3-5 cultures and 22% of P16-18 cultures, at DIV7. $SOX9^+$ are predominantly co-expressed with vimentin and are highest at DIV16 of P3-5 cultures, correlating to gliogenesis initiation.
6. Vimentin stains more astrocytes than GFAP in opossum cultures. Every $GFAP^+$ cell is vim^+ in P3-5 cultures, while $GFAP^+vim^-$ cells are present in P16-18 cultures. *In vitro* astrocyte maturation proceeds with vimentin downregulation.
7. *In vitro* maturation of cortical primary cell cultures has a similar time-line of maturation as *in vivo* maturation of opossum cortex.
8. Spontaneous calcium activity is observed in DIV7 of P3-5 and P16-18 cultures. Synchronicity in cell activity is visible.
9. 48 hours after an injury in P3-5 and P16-18 cultures, connections between the injury sides are formed. Astrocytes accumulate around the injury and migrate inside the injury area.

10. 24 hours after an injury in DIV10 P16-18 cultures, a reduction of injury size is observed, as well as glial-scar-like formation. The same is observed 48 hours after an injury in DIV10 P3-5 cultures.
11. 24 hours after injury performed in DIV14 P3-5 opossums, numerous connections are formed between the opposite sides of the injury. Connections are significantly more prominent than in P16-18 cultures.
12. In DIV10 P3-5 cultures, 48 hours after an injury, striking calcium activity pattern is observed. 72 hours after an injury, two patterns of calcium activity are observed. A cell migrated across injury area and showed calcium activity pattern of cells from the opposite side of the injury.

7. References

1. Werner, C. & Engelhard, K. Pathophysiology of traumatic brain injury. *British Journal of Anaesthesia* (2007) doi:10.1093/bja/aem131.

2. Wang, H. *et al.* Portrait of glial scar in neurological diseases. *Int. J. Immunopathol. Pharmacol.* **31**, 1–6 (2018).

3. Silver, J. & Miller, J. H. Regeneration beyond the glial scar. *Nature Reviews Neuroscience* (2004) doi:10.1038/nrn1326.

4. Duan, C. L. *et al.* Striatal astrocytes transdifferentiate into functional mature neurons following ischemic brain injury. *Glia* **63**, 1660–1670 (2015).

5. Chuckowree, J. A., Dickson, T. C. & Vickers, J. C. Intrinsic regenerative ability of mature CNS neurons. *Neuroscientist* **10**, 280–285 (2004).

6. Martínez-Cerdeño, V. & Noctor, S. C. Neural progenitor cell terminology. *Front. Neuroanat.* **12**, 1–8 (2018).

7. Emsley, J. G., Mitchell, B. D., Kempermann, G. & Macklis, J. D. Adult neurogenesis and repair of the adult CNS with neural progenitors, precursors, and stem cells. *Prog. Neurobiol.* **75**, 321–341 (2005).

8. Arai, K. & Lo, E. H. Gliogenesis. *Prim. Cerebrovasc. Dis. Second Ed.* 91–95 (2017) doi:10.1016/B978-0-12-803058-5.00018-7.

9. Palmer, T. D., Markakis, E. A., Willhoite, A. R., Safar, F. & Gage, F. H. Fibroblast growth factor-2 activates a latent neurogenic program in neural stem cells ’from diverse regions of the adult CNS. *J. Neurosci.* **19**, 8487–8497 (1999).

10. Lie, D. C. *et al.* The adult substantia nigra contains progenitor cells with neurogenic potential. *J. Neurosci.* **22**, 6639–6649 (2002).

11. Bernier, P. J., Bédard, A., Vinet, J., Lévesque, M. & Parent, A. Newly generated neurons in the amygdala and adjoining cortex of adult primates. *Proc. Natl. Acad. Sci. U. S. A.* **99**, 11464–11469 (2002).

12. Götz, M., Hartfuss, E. & Malatesta, P. Radial glial cells as neuronal precursors: A new perspective on the correlation of morphology and lineage restriction in the developing cerebral cortex of mice. *Brain Res. Bull.* **57**, 777–788 (2002).

13. Mori, T., Buffo, A. & Götz, M. The Novel Roles of Glial Cells Revisited: The Contribution of Radial Glia and Astrocytes to Neurogenesis. *Curr. Top. Dev. Biol.* **69**, 67–99 (2005).

14. Eisch, A. J., Barrot, M., Schad, C. A., Self, D. W. & Nestler, E. J. Opiates inhibit neurogenesis in the adult rat hippocampus. *Proc. Natl. Acad. Sci. U. S. A.* **97**, 7579–7584 (2000).

15. Gould, E. & Tanapat, P. Stress and hippocampal neurogenesis. *Biol. Psychiatry* **46**, 1472–1479 (1999).

16. Yau, S. Y., Gil-Mohapel, J., Christie, B. R. & So, K. F. Physical exercise-induced adult neurogenesis: A good strategy to prevent cognitive decline in neurodegenerative diseases? *Biomed Res. Int.* **2014**, (2014).

17. Ramaswamy, S., Goings, G. E., Soderstrom, K. E., Szele, F. G. & Kozlowski, D. A. Cellular proliferation and migration following a controlled cortical impact in the mouse. *Brain Res.* **1053**, 38–53 (2005).

18. Dash, P. K., Mach, S. A. & Moore, A. N. Enhanced neurogenesis in the rodent following traumatic brain injury. *J. Neurosci. Res.* **63**, 313–319 (2001).

19. Chirumamilla, S., Sun, D., Bullock, M. R. & Colello, R. J. Traumatic brain injury induced cell proliferation in the adult mammalian central

nervous system. *J. Neurotrauma* **19**, 693–703 (2002).

20. David, S. & Aguayo, A. J. Axonal elongation into peripheral nervous system 'bridges' after central nervous system injury in adult rats. *Science (80-.).* **214**, 931–933 (1981).

21. Eric A. Huebner, S. M. S. Smelling, Tasting, Learning: *Results Probl Cell Differ.* 339–351 (2009) doi:10.1007/400.

22. Yiu, G. & He, Z. Glial inhibition of CNS axon regeneration. *Nat. Rev. Neurosci.* **7**, 617–627 (2006).

23. He, Z. & Jin, Y. Intrinsic Control of Axon Regeneration. *Neuron* **90**, 437–451 (2016).

24. Blankenship, A. G. & Feller, M. B. Mechanisms underlying spontaneous patterned activity in developing neural circuits. *Nat. Rev. Neurosci.* **11**, 18–29 (2010).

25. Rosenberg, S. S. & Spitzer, N. C. Calcium signaling in neuronal development. *Cold Spring Harb. Perspect. Biol.* **3**, 1–13 (2011).

26. Spitzer, N. C., Olson, E. & Gu, X. Spontaneous calcium transients regulate neuronal plasticity in developing neurons. *J. Neurobiol.* **26**, 316–324 (1995).

27. Rehder, V., Jensen, J. R. & Kater, S. B. The initial stages of neural regeneration are dependent upon intracellular calcium levels. *Neuroscience* **51**, 565–574 (1992).

28. Zhang, J. & Jiao, J. Molecular Biomarkers for Embryonic and Adult Neural Stem Cell and Neurogenesis. *Biomed Res. Int.* **2015**, (2015).

29. Gómez-López, S. *et al.* Sox2 and Pax6 maintain the proliferative and developmental potential of gliogenic neural stem cells in vitro. *Glia* **59**, 1588–1599 (2011).

30. Hutton, S. R. & Pevny, L. H. SOX2 expression levels distinguish between neural progenitor populations of the developing dorsal telencephalon. *Dev. Biol.* **352**, 40–47 (2011).

31. Hoffmann, S. A. *et al.* Stem cell factor Sox2 and its close relative Sox3 have differentiation functions in oligodendrocytes. *Dev.* **141**, 39–50 (2014).

32. Niu, W. *et al.* In vivo reprogramming of astrocytes to neuroblasts in the adult brain. *Nat. Cell Biol.* **15**, 1164–1175 (2013).

33. Gu, J. *et al.* The expression of NP847 and sox2 after TBI and its influence on NSCs. *Front. Cell. Neurosci.* **10**, 1–12 (2016).

34. Bramanti, V., Tomassoni, D., Avitabile, M., Amenta, F. & Avola, R. Biomarkers of glial cell proliferation and differentiation in culture. *Front. Biosci. - Sch.* **2 S**, 558–570 (2010).

35. Jiang, Y. Q. & Oblinger, M. M. Differential regulation of β(III) and other tubulin genes during peripheral and central neuron development. *J. Cell Sci.* **103**, 643–651 (1992).

36. Scott, C. E. *et al.* SOX9 induces and maintains neural stem cells. *Nat. Neurosci.* **13**, 1181–1189 (2010).

37. Kang, P. *et al.* Sox9 and NFIA Coordinate a Transcriptional Regulatory Cascade during the Initiation of Gliogenesis. *Neuron* **74**, 79–94 (2012).

38. Nicholls, J. G., Stewart, R. R., Erulkar, S. D. & Saunders, N. R. Reflexes, fictive respiration and cell division in the brain and spinal cord of the newborn opossum, Monodelphis domestica, isolated and maintained in vitro. *J. Exp. Biol.* **152**, 1–15 (1990).

39. Cardoso-Moreira, M. *et al.* Gene expression across mammalian organ development. *Nature* **571**, 505–509 (2019).

40. Puzzolo, E. & Mallamaci, A. Cortico-cerebral histogenesis in the opossum Monodelphis domestica: Generation of a hexalaminar neocortex in the absence of a basal proliferative compartment. *Neural Dev.* **5**, 1–18 (2010).

41. Nicholls, J. & Saunders, N. Regeneration of immature mammalian spinal cord after injury. *Trends Neurosci.* **19**, 229–234 (1996).

42. Wintzer, M. *et al.* Strategies for identifying genes that play a role in spinal cord regeneration. *J. Anat.* **204**, 3–11 (2004).

43. Lane, M. A. *et al.* Age-related differences in the local cellular and molecular responses to injury in developing spinal cord of the opossum, Monodelphis domestica. *Eur. J. Neurosci.* **25**, 1725–1742 (2007).

44. Petrović, A. *et al.* Establishment of Long-Term Primary Cortical Neuronal Cultures From Neonatal Opossum Monodelphis domestica. *Front. Cell. Neurosci.* (2021) doi:10.3389/fncel.2021.661492.

45. Beaudoin, G. M. J. *et al.* Culturing pyramidal neurons from the early postnatal mouse hippocampus and cortex. *Nat. Protoc.* (2012) doi:10.1038/nprot.2012.099.

46. Von Bohlen Und Halbach, O. Immunohistological markers for proliferative events, gliogenesis, and neurogenesis within the adult hippocampus. *Cell Tissue Res.* **345**, 1–19 (2011).

47. Rizzuto, R. *et al.* Calcium and apoptosis: Facts and hypotheses. *Oncogene* **22**, 8619–8627 (2003).

48. Ellis, P. *et al.* SOX2, a persistent marker for multipotential neural stem cells derived from embryonic stem cells, the embryo or the adult. *Dev. Neurosci.* **26**, 148–165 (2004).

49. Sun, W. *et al.* SOX9 is an astrocyte-specific nuclear marker in the adult

brain outside the neurogenic regions. *J. Neurosci.* **37**, 4493–4507 (2017).

50. Bootman, M. D., Rietdorf, K., Collins, T., Walker, S. & Sanderson, M. Ca2+-sensitive fluorescent dyes and intracellular Ca2+ imaging. *Cold Spring Harb. Protoc.* **8**, 83–99 (2013).

51. Chen, C. *et al.* Astrocyte-Specific Deletion of Sox2 Promotes Functional Recovery after Traumatic Brain Injury. *Cereb. Cortex* **29**, 54–69 (2019).

Financial support

The experimental work has been conducted on equipment financed by the European Regional Development Fund (ERDF) within the project "Research Infrastructure for Campus-based Laboratories at University of Rijeka" (RC.2.2.06-0001), the Croatian Science Foundation (CSF) grant IP-2016-06-7060 and the financial support from the University of Rijeka (18-258-6427 and 18-290-1463).